공학석사학위논문

Surface-Charged PVDF Membrane via Assembly of Charged Hyperbranched Polyglycerol (HPG) for Suppression of Membrane Fouling

전하를 도입한 고차가지구조 폴리글리세롤(HPG)의

PVDF 분리막 표면개질에 의한 오염 저감 영향에 대한 연구

2015 년 2 월

서울대학교 대학원

재료공학부

김 예 지

Surface-Charged PVDF Membrane via Assembly of Charged Hyperbranched Polyglycerol (HPG) for Suppression of Membrane Fouling

전하를 도입한 고차가지구조 폴리글리세롤(HPG)의
PVDF 분리막 표면개질에 의한 오염저감 영향에 대한 연구

지도 교수 곽 승 엽

이 논문을 공학석사 학위논문으로 제출함
2014 년 12 월

서울대학교 대학원
재료공학부
김 예 지

김예지의 공학석사 학위논문을 인준함
2014 년 12 월

위 원 장 장 지 영 (인)
부위원장 곽 승 엽 (인)
위 원 김 재 필 (인)

ABSTRACT

Surface-Charged PVDF Membrane via Assembly of Charged Hyperbranched Polyglycerol (HPG) for Suppression of Membrane Fouling

Kim Ye Ji

Department of Materials Science And Engineering

The Graduate School

Seoul National University

Surface charged polyvinylidene fluoride (PVDF) ultra/micro (UF/MF) filtration membranes were prepared by covalent assembly of various charged hyperbranched polyglycerol (HPG) to endow fouling resistance against numerous charged water contaminants. First, we prepared three types of charged HPG, *i.e.*, neutral, positive, negative charges, by end-group modification. Next, PVDF flat membranes were treated with plasma irradiation to introduce functional groups, such as O-O, -OOH, -NH_2, CONH, etc. Finally, the charged HPG was covalently bonded with the modified membrane surface using phenylene diisocyanate as a linking agent. Successful polymerization and charged modification of HPGs were

examined by combined results of Fourier transform infrared (FT-IR) and proton nuclear magnetic resonance (^{1}H-NMR). Attenuated total reflectance (ATR) FT-IR and X-ray photoelectron spectroscopy (XPS) spectra detected addition of the neutral HPG and charged HPGs on the surface of the charge-modified membrane. Enhancement of hydrophilic property of charge-modified membrane without severe change of their morphology was observed by analysis of water contact angle (CA) and field emission scanning electron microscope (FE-SEM). Charge characteristic of membranes were detected by ion exchange capacity (IEC) and zeta potential analysis, revealed successful charge modification. Assessment of anti-fouling property was conducted by charged proteins (bovine serum albumin and lysozyme) contained water. These results indicated that hydrophilic property and electrostatic repulsive force between charged membrane surface and identical charged contaminants decreased foulants adsorption on membrane surface. Therefore, positively or negatively charge-modified membranes exhibited best antifouling performance to co-ionized protein solution. Likewise, the neutral charge-modified membrane showed intermediate performance to both protein solutions. In addition, the charge-modified membranes occurs adsorption of counter charged proteins, which can improve charged protein separation. Thus, membrane surface modification with charged HPG makes eco-friendly membrane, that might be used as application of various wastewater and charged particle-separation.

Keywords

Charge modification, Hyperbranched polyglycerol (HPG), PVDF membrane, Antifouling, Protein separation

***Student number*: 2013-20588**

CONTENTS

1. Introduction

Low pressurized membrane processes such as ultra/micro (UF/MF) filtration membrane can effectively purified contaminated water by removal of small pollutants such as colloidal particles, microorganisms and so on. They are well used for wastewater and drinking water treatment. It is widely used materials to fabricate UF/MF membrane that has excellent chemical resistance, good thermal property, *e.g.*, Polyvinylidene fluoride (PVDF), polytetrafuloroethylene (PTFE), polypropylene (PP), polysulfone (PSF), polyacrylonitrile (PAN) and so forth [1-4]. Nevertheless, due to hydrophobic property of those polymer membranes, they are prone to fouling. Hydrophobic organic molecules are prone to drive toward the hydrophobic membrane surface, so it occurs an adsorption of retained matters such as proteins, salts, particles, and the rest on the membrane surface and pores, that lead the reduction of the membrane performance [5]. The lots of contaminants in wastewater have not only hydrophobic nature, but also localized charge. Therefore, increase of membrane surfaces hydrophilic property and charge property can reduce membrane fouling due to reduction of hydrophobic interaction on hydrophilic modified-membranes and charge repulsion between co-ionized membranes surface and foulants.

Various methods have been established to give the conventional hydrophobic polymeric membranes with hydrophilic properties. These

approaches can be classified in to the surface coating, surface grafting hydrophilic monomer polymerization [2, 5-9]. However, coating and grafting modification methods may have some disadvantages, eroding of coating layer or block membrane pores by monomer grafting methods [10]. Furthermore, direct graft polymerization on membrane surface usually requires harsh conditions such as high reaction temperature, severe pH condition and so on. In particular, method of grafting-onto already polymerized hydrophilic polymer using linker agent is a highly efficient that offers mild processing condition, one to one reaction with high reactivity, and no inessential side products [2]. To graft linker on PVDF membrane, it should be activated by a gas plasma, ozone, UV, or ion irradiation to introduce the functional groups [2, 11]. Especially, low temperature plasma surface modification may extremely attractive technique due to preservability of the mechanical and physicochemical properties during modification process. In recent year, atmospheric-pressure plasma were widely used because they has advantages such as dry process and pollution control unlike low pressure plasma [11, 12].

Among grafting hydrophilic polymer onto membrane surface, polyethylene glycol (PEG) is used widely, due to its high hydrophilic property [2, 13, 14]. Hyperbranched polyglycerol (HPG) has advantages of PEG and structural forms, such as high density, low viscosity, and multiple end functionalities of high reactive and hydrophilic hydroxyl groups [15, 16].

Methods of charge providing modification as well as hydrophilic property endowing modification are also efficient to reduce fouling on membrane surface. [5, 17, 18]. Positively or negatively charged membranes have hydrophilic properties that acquired by strong capacity to generate a hydration layer via electrostatic interaction between ions and water molecules. Moreover, between charged surface and the charged matter in the feed solution, electrostatic repulsion forces works to prevent the solute adsorption on the membrane surface. Many researchers studied charged membranes, using various modifying methods [18-26, 42-43, 47-49]. The number of researchers suggested that negative charge modification were done by blends of polysulfone and sulfonated poly(ether, ether ketone) [18, 19]. High rejection property of humic acid and low fouling properties were seen at these membranes. In addition, negatively charged membrane can easily rinse out foulants, such as negatively charged humic acid deposits [21]. Jin Zhan et al. [20] reported positively charged monomer grafted membrane reduces adsorption of positively charged lysozyme and negatively charged acrylic acid monomer grafted membrane reduces negatively charged bovine serum albumin adsorption. However, grafting to methods using charged monomers could not control polymerization degree, so fouling extent by structure of polymer was not accounted. Matsumoto et al. [24] analyzed anti-fouling performance of charged-membranes, which were grafted by already synthesized charged polymers. Due to the same structure of linked polymer, charge difference was the only variables that

occurs dissimilar fouling performance. Nevertheless, fouling performance of neutral charged membranes, grafted by the neutral charged polymer of the same structure was not observed. Furthermore, anti-fouling performance was detected by adsorption test only, so further study is demanded to analyze fouling resistance of charged membranes by filtration test.

In this study, we figured out anti-fouling properties of various charge-modified membranes by assembly of various charged HPG derivatives. Using neutral charged HPG as hydrophilic backbone, add charged matter on HPG to control positive, neutral, or negative charge effect and to minimize alteration of polymer structure. First, HPG was polymerized using glycidol as monomer. Next, end-group modification of HPG was carried out by introducing positive or negative charge. Finally, various charged membranes were prepared by covalent assembly of various charged HPG. The charge-modified membranes have been evaluated in the selective transport of the model protein bovine serum albumin (BSA) lysozyme (Lyz) solution at pH 7.4. In addition, to evaluate the separation property for charge-modified membrane, transport of protein separation test was conducted using the hemoglobin-bovine serum albumin mixture. As expected, electrostatic repulsion between charged membrane and co-ionized proteins improved anti-fouling property at fouling test. In addition, separation efficiency was slightly increased due to electrostatic adsorption. Therefore, charge-modified membranes can be used at application of various wastewater treatment and charged particle-separation.

2. Experimental

2.1. Materials

Bz_2THAM: benzyl bromide (≥ 99.0%, Alfa Aesar), tris(hydroxymethyl)aminomethane (THAM, ≥ 99.8%, Sigma-Aldrich), potassium carbonate (K_2CO_3, anhydrous, ≥ 99.5%, DAEJUNG), N,N-dimethylformamide (DMF, ≥ 99.8%, DAEJUNG), chloroform ($CHCl_3$, 99.5%, DAEJUNG), sodium hydrogen carbonate ($NaHCO_3$, 99%, DEAJUNG), magnesium sulfate ($MgSO_4$, anhydrous, ≥ 99%, DAEJUNG), ethyl acetate (99.9%, Sigma-Aldrich), DI water by pure power Ⅲ, hanascience (Korea).

Bz_2-HPG: cesium hydroxide monohydrate (100%, Sigma-Aldrich), benzene (≥ 99.5%, DAEJUNG), diethylene glycol dimethyl ether (diglyme, 99.5%, Sigma-Aldrich), glycidol (≥ 96.0%, Sigma-Aldrich), 5 N hydrochloric acid (HCl, DAEJUNG), diethyl ether (99%, DAEJUNG)

Debenzylation: ethanol (99%, anhydrous, DAEJUNG), acetic acid (≥ 99.0%, Sigma-Aldrich), palladium on carbon (pd/c, 10 wt%, Sigma-Aldrich), celite pad (Sigma-Aldrich)

Charged HPG: sodium hydroxide (NaOH, 98%, DAEJUNG), glycidyl trimethylammonium chloride (GTA, ≥ 90.0%, Sigma-Aldrich), methanol (≥

99.5%, DAEJUNG), filter paper by ADVANTEC (5C, 70mm, 100 circles, U.S.A.), sulfur trioxide pyridine complex (STPC, 98.0%, Sigma-Aldrich), 1 N sodium hydroxide solution (DAEJUNG), acetone (≥ 99.5%, DAEJUNG)

Modification of membrane: durapore hydrophobic PVDF membrane filter, PPHP04700 (pore size 0.1 μm), 1,4-phenylene diisocyanate (PDC, Sigma-Aldrich), toluene (99.8%, anhydrous, Sigma-Aldrich), dibutyltin dilaurate (DBTL, ≥ 95.0%, Aldrich), 0.1 N NaOH solution (DAEJUNG), 0.1 N HCl solution (DAEJUNG), sodium chloride (DAEJUNG).

Evaluation of membrane performance: PBS ingredients; potassium chloride (KCl, ≥ 99.8%, Sigma-Aldrich), sodium phosphate dibasic (Na_2HPO_4, ≥ 99.0%, Sigma-Aldrich), potassium phosphate monobasic (KH_2PO_4, ≥ 99.0%, Sigma-Aldrich), acetate buffer ingredients; acetic acid (≥ 99.0%, Sigma-Aldrich), sodium acetate ($C_2H_3O_2Na$, ≥ 99.0%, Sigma-Aldrich), lysozyme (Lyz, Sigma-Aldrich), bovine serum albumin (BSA, Bovogen), hemoglobin from bovine blood (Hb, Sigma-Aldrich), durapore hydrophilic PVDF membrane filter, PPLP04700 (pore size 0.1 μm).

2.2. Synthesis of hyperbranched polyglycerol with precisely one focal amino functionality (NH_2-HPG)

2.2.1 Synthesis of N,N-dibenzyl tris(hydroxymethyl) aminomethane (Bz_2THAM)

The introduction of the benzyl group on THAM was conducted according to a slightly modified, previously reported method [27]. A mixture of 34 g of benzyl bromide (0.2mol), 11 g (0.09 mol) of tris(hydroxymethyl) aminomethane (THAM), 27.6 g of K_2CO_3 (100 mM), and 150 mL of DMF were refluxed at 105 ℃ for 24 h. After cooling the reaction mixture at room temperature, the solution was filtrated and DMF was removed in vacuo at 85 ℃ for 3 h. Then, 150 mL of $CHCl_3$ were added, and the solution was rinsed with saturated $NaHCO_3$ solution (2 × 200 mL) and water (200 mL) and dried with $MgSO_4$. The solvent was removed using evaporator, and a highly viscous, slightly yellow liquid was obtained. The crude product mixture was refined by recrystallization from ethyl acetate, giving a white solid of the desired product that was dried under vacuum. Proton Nuclear Magnetic Resonance (^{1}H-NMR) was measured to determine presence of above reaction with an Avance 600, high resolution NMR spectrometer by Bruker (Germany). (600 MHz, DMSO-d6): δ (ppm) = 7.28−7.02 (10H, aromatic), 4.34−4.26 (3H, OH), 3.99−3.91 (4H, $PhCNH_2$), 3.55−3.45 (6H, CCH_2OH). See Figure 9.

2.2.2 Synthesis of N,N-dibenzyl tris(hydroxymethyl) aminomethane initiated hyperbranched polyglycerol (Bz_2-HPG)

The 6.03 g sample of Bz_2THAM (0.02mol), and 1.01 g Cesium hydroxide monohydrate (10%, 0.006mol) were dissolved in benzene at 73 ℃. The solution was stirred for 1 h at room temperature and the solvents were removed in vacuo at 90 ℃. The initiator powder was dissolved in diglyme and a 31.20 g of glycidol was added slowly (rate: 0.02 mL/min) using a syringe pump by KD scientific, legate pump (U.S.A.) at 100 ℃. The highly viscous product was dissolved in methanol in order to terminate reaction. After that, 1.2 mL 5 N HCl solution was added, concentrated, and precipitated into cold diethyl ether. Yields: 90%. ^{1}H-NMR (600 MHz, D_2O): δ (ppm) = 7.47−7.16 (10H, aromatic), 4.90−4.70 (D_2O, OH), 4.1−3.25 (polyether backbone). See Figure 11.

2.2.3. Deprotection to hyperbranched polyglycerol analogues with exactly one amino group (NH_2-HPG).

The debenzylation was managed consistent with a little altered, previously reported approaches [28]. A 5 g sample of Bz_2-HPG was dissolved in 130 mL ethanol, 1.3 mL acetic acid and 0.8 g of Pd/C was added. The reaction vessel was flushed with hydrogen (1 atm) and the reaction was allowed to stir for 14 h at 60 ℃. The solution was filtered by

celite pad, solvent removed by evaporator, subsequently dried for 24 h at 80 ℃. Yields: 67%. ^{1}H-NMR (600 MHz, D_2O): δ (ppm) = 4.90−4.70 (D_2O, OH), 4.09-3.52 (polyether backbone). See Figure 11.

2.3. Synthesis of positively charged hyperbranched polyglycerol (NH_2-PHPG)

2.3.1 Synthesis of Benzyl protected quarternized ammonium hyperbranched polyglycerol (Bz_2-PHPG)

The 11.03 g sample of Bz_2-HPG (1eq) and 13.69 g of NaOH (2.4 equiv.; OH of Bz_2-HPG) were added in 60 mL DI water. The solution was cooled at ~0 ℃ and reacted with 25.94 g of glycidyl trimethylammonium chloride (GTA, 1.2 equiv.; OH of Bz_2-HPG) which were added drop wise. The mixture was reacted 16 h and subsequently neutralized with 68.42 mL 5N HCl. The solvent was removed by evaporator at 60 ℃ and dissolved in methanol for precipitating NaCl, which was removed by filtration. The filtrated solvent was distilled off at 60 ℃ and dried for 24 h at 60 ℃. The introduction of the quaternary ammonium and degree of substitution was identified by ^{1}H-NMR (600 MHz, D_2O) δ: 7.47−7.16 (10H, aromatic), 4.90−4.70 (D_2O, OH), 4.35 (^{1}H, $CHOHCH_2N^{+}(CH_3)_3$), 4.03–3.27 (polyether backbone), 3.16 (3H, $N^{+}(CH_3)_3$) [29].

2.3.2. Deprotection to positively charged hyperbranched polyglycerol analogues with exactly one amino group (NH_2-PHPG)

The debenzylation was conducted similarly according to the procedure of 2.2.3. The 5 g of Bz_2-HPG dissolved in 60 mL ethanol, then filtrating NaCl one more time. Adding Pd/C at room temperature, subsequently raise the temperature slowly to prevent explosion. Yields: ~90%. See Figure 11.

2.4. Synthesis of negatively charged hyperbranched polyglycerol (NH_2-NHPG)

2.4.1. Synthesis of benzyl protected hyperbranched polyglycerol sulfate (Bz_2-NHPG)

A solution of STPC (11.44 g, 71.2 mM) in 80 mL DMF was added dropwise to a solution of Bz_2-HPG (5.508 g, 71.2 mM OH-groups) in 50 mL DMF over 6 h at 60 ℃ (drop wise rate: 0.11 mL/min). After the solution was stirred for an extra 4 h at 60 ℃ and 24 h at room temperature, subsequently water (13 mL) was added. Adding aqueous NaOH (1 M) to the resulting mixture until a pH 11 was reached. The solvent was evaporated in vacuo at 90 ℃, which gave the crude product. That precipitated at cooled

acetone twice. The solvent was removed by evaporator at 60 ℃ to give NH_2-NHPG as a pale yellow solid. ^{1}H NMR (600 MHz, D_2O): δ (ppm) = 7.70−7.00 (10H, aromatic), 4.90−4.760 (D_2O, OH), 4.24–4.75 (m, -$OCH_2CH(OSO_3Na)$, CH_2OSO_3Na) 3.50–4.2 (polyether backbone). IR (KBr, cm^{-1}): 3443 (OH), 2924 (CH), 1259 (S=O), 805 (C–O–S) [30].

2.4.2. Deprotection to negatively charged hyperbranched polyglycerol analogues with exactly one amino group (NH_2-NHPG)

The 4.67 g sample of Bz_2-NHPG was dissolved in 100 mL DI water and 100 mL ethanol at 60 ℃. At room temperature, 4 mL acetic acid and 1.5 g of Pd/C were added. The reaction vessel was flushed with hydrogen (1 atm) and the reaction was allowed to stir for 4 days at 60 ℃. The solution was filtered by celite pad, solvent removed by evaporator, subsequently dried for 24 h at 80 ℃.), ^{1}H NMR (600 MHz, D_2O): δ (ppm) = 4.90−4.760 (D_2O, OH), 4.24–4.75 (m, -$OCH_2CH(OSO_3Na)CH_2OSO_3Na$) 3.50–4.2 (polyether backbone). See Figure 11.

2.5. Surface modification of PVDF membrane by NH_2(EG)HPG

2.5.1. Introduction of functional group into PVDF membrane by plasma treatment

Plasma treatment was carried out with a Myple-2000 (Korea) on PVDF membrane fixed by stainless frame. The sample is mounted on table with 4.5 mm distance away from plasma glow. An electrical field is applied to ignite the plasma glow discharge by a 13.56 MHz radio frequency power supply. The membrane were argon (carrier gas) and Oxygen (reaction gas) plasma treated at a radio-frequency power of 100 W for 4 min. Argon gas flow was 8 cm^3/min and that of oxygen was 20 cm^3/min. Subsequently, the membrane were exposed to air for 30 min

2.5.2. Grafting NH_2(EG)HPG onto the PVDF membrane by cross linking agent

The 0.92 g of cross linker PDC was dissolved in 123.5 mL toluene at room temperature. The air exposed PVDF membrane were immersed in PDC solution, subsequently 6.5 mL DBTL (5 wt%) were added. The sample were placed on a shaking incubator BF-30.SI made by Biofree (Korea) at 130 rpm and 37 ℃ for 3 h. The reacted membrane were washed with toluene and dipped in a 10 wt% solution of NH_2-HPG, NH_2-PHPG, NH_2-

NHPG in ethanol, which was added 0.1 wt% DBTL. Those were shaken at 150 rpm and 27.7 ℃ for 24 h. The HPG and charged HPG linked membranes were washed with ethanol and DI water for three times to remove unreacted polymer and dried off solvent at room temperature.

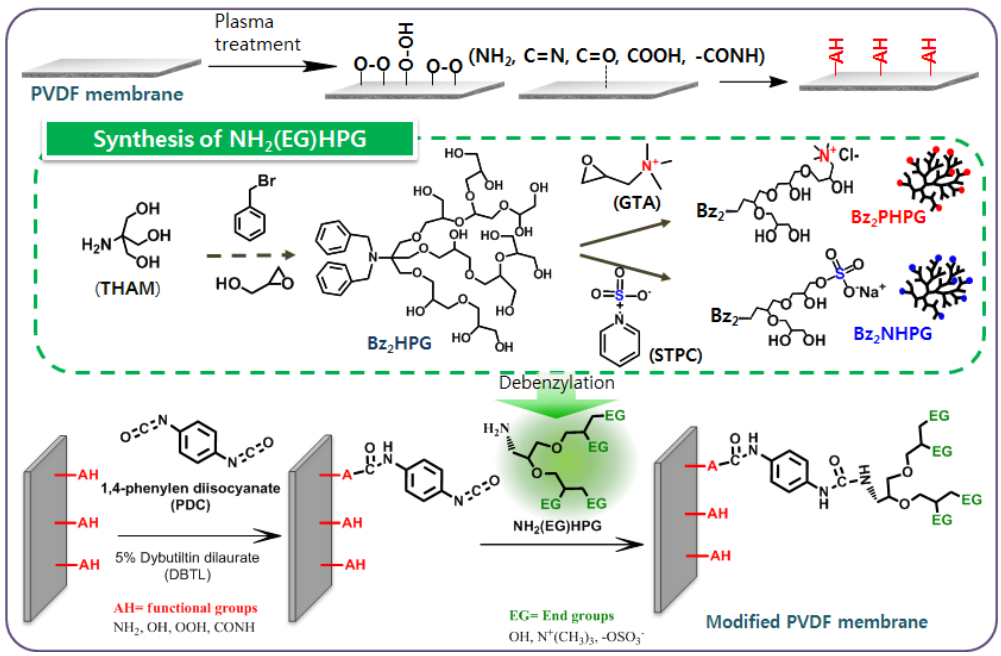

Figure 1. Schematic illustration of surface modification of PVDF membrane by NH_2(EG)HPG

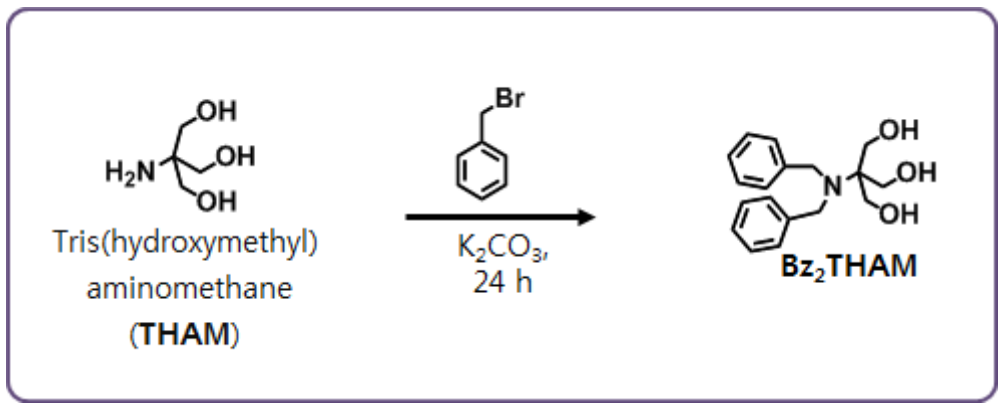

Figure 2. Synthesis of *N,N*-dibenzyl tris(hydroxymethyl) aminomethane (Bz_2THAM)

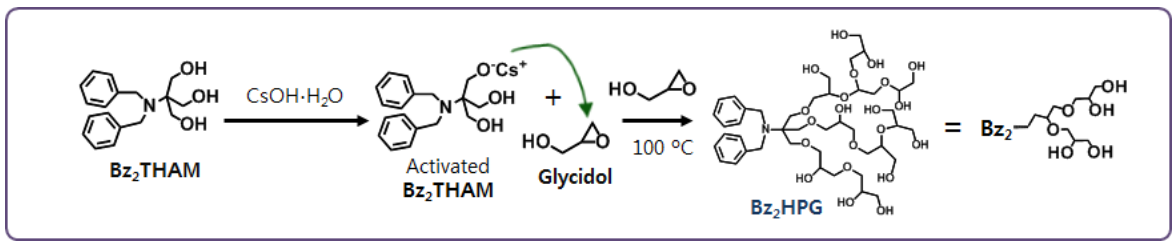

Figure 3. Polymerization of *N,N*-dibenzyl protected HPG (Bz_2-HPG)

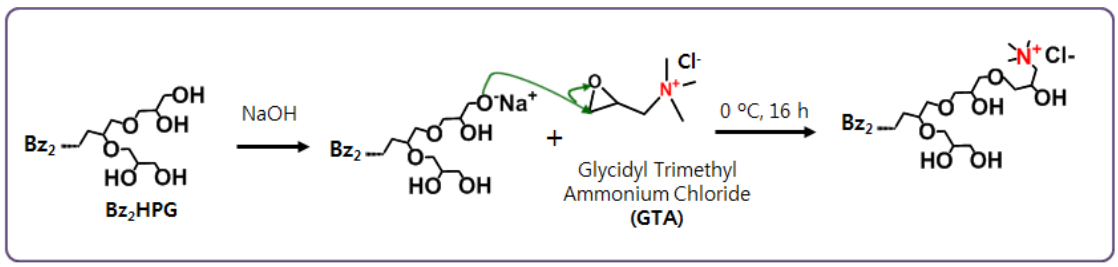

Figure 4. Modification of Bz_2-HPG by positively charged matters

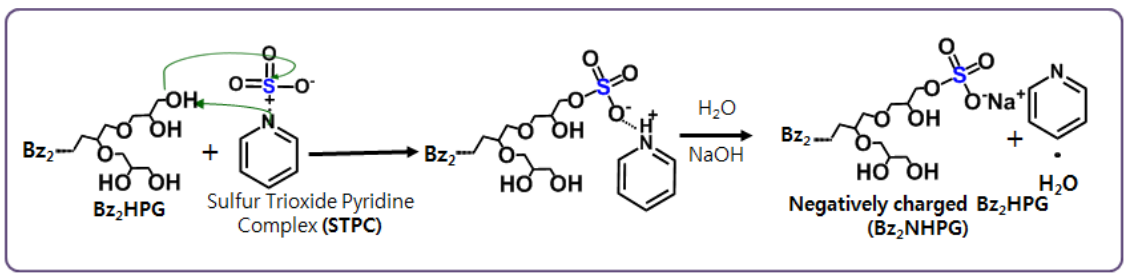

Figure 5. Modification of Bz_2-HPG by negatively charged matters

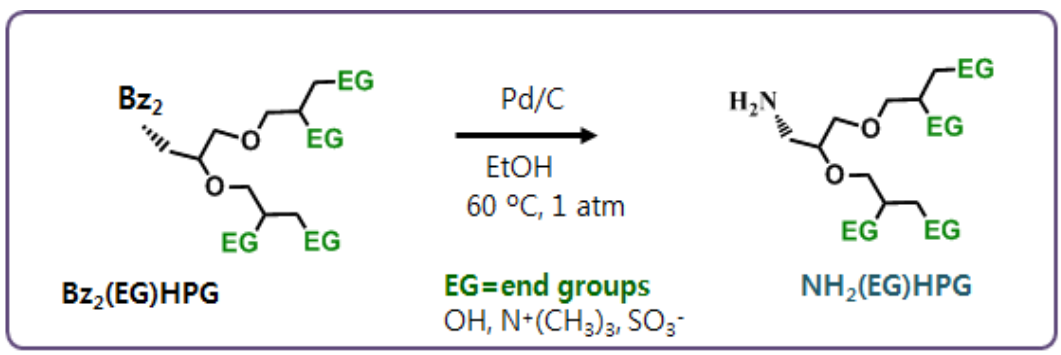

Figure 6. Deprotection to HPG with exactly one amino group

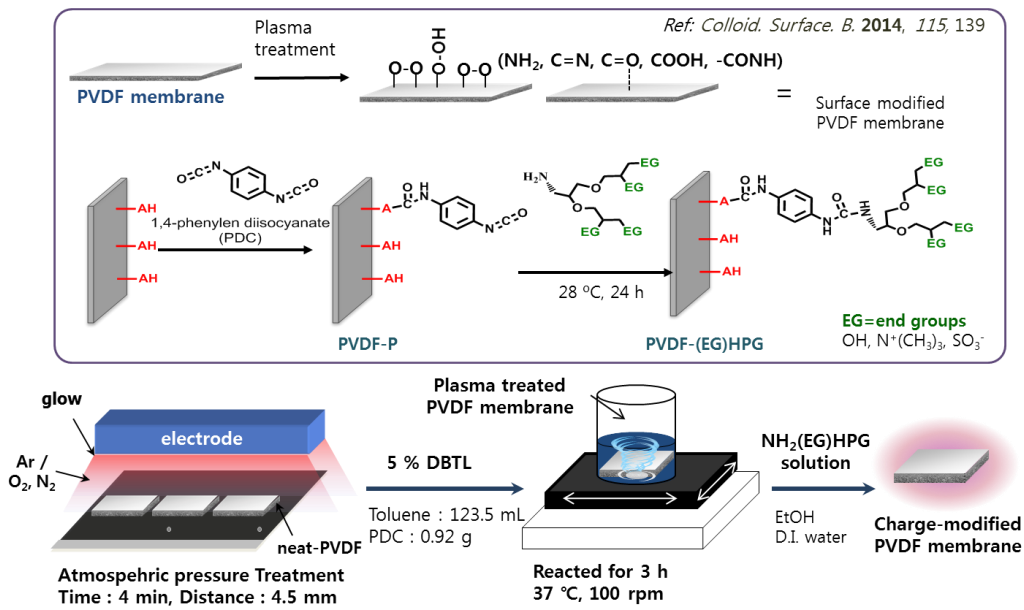

Figure 7. Surface modification of PVDF membrane by PDC and NH_2(EG)HPG

2.6. Characteristics of membranes

2.6.1. Analysis of surface chemical compositions

The surface chemical composition of the membranes was characterized by ATR-IR and XPS. IR spectroscopic investigation was carried out with a Nicolet 6700 attenuated total reflectance infrared (ATR-IR) spectrometer. Spectra were recorded in air in the ATR mode using a zinc selenite tip.

X-ray photoelectron spectroscopy (XPS) was recorded on an Axis-HSI by Kratos (U.K.). It has material Mg/Al dual anode but use magnesium as anode material. X-ray power was 10 mA and 15 kV and its detector was 45° away from the normal. It has 127 mm mean radius hemispherical analyzer, five multi-channel detection system, co-axial charge neutralization. Pass energy of XPS was 20 eV and Energy resolution of this was 0.1 eV.

Contact angles were measured by the Attention® THETA LITE, BiolinScientific (Sweden) using DI water at room temperature. Interaction between the DI water and surface of membrane can be attractive when it has hydrophilic property or repulsive when it has hydrophobic property.

2.6.2. Membrane morphology

Surface morphologies of the PVDF membrane and charge-modified PVDF membrane were studied by JSM-7600 scanning electron microscope, JEOL (Japan) under the standard high-vacuum conditions with and accelerating voltage of 0.1-30 kV. Each sample was dried under vacuum and mounted on the stage by means of double-sided adhesive carbon tapes. After this, samples were coated with platinum by a vacuum electric sputter coater, prior FE-SEM analysis.

2.6.3. Ion-exchange capacity (IEC) determination

Ion-exchange capacity (IEC) was determined similarly according to the previous method [31, 32].

The IEC of positively charged membranes

Accurately weighed (W_d) membrane was wetted at ethanol, subsequently filtrated 1 litter of DI water for fully wetting. The sample was immersed in 0.1 N NaOH solution for 24 h to exchange Cl^- into OH^- form. The sample was washed with DI water to remove any excess base. After that, it was immersed in a 50 mL 0.1 N HCl solution for 24 h. Exchanged amount of OH^- was determined by back titration with 0.1 N NaOH solution in the membrane soaked 50 mL HCl solution, using phenolphthalein as a colorimetric indicator. The IEC value (meq/g) was then calculated as the ratio of the titrated amount of OH^- to the weight of the dried membrane. See

equation (1) where V_{HCl} is the volume of HCl solution (50 mL), V_{NaOH}, the volume of the NaOH solution consumed in the back titration, N_{HCl} the normality of HCl (0.1 N) and , N_{NaOH} the normality of NaOH (0.1 N) W_d is the weight of dry membrane (g).

$$\text{IEC}\left(\frac{\text{meq}}{\text{g}}\right) = [V_{HCl} \cdot N_{HCl} - V_{NaOH} \cdot N_{NaOH}]/W_d \quad \text{..... (1)}$$

The IEC of neutral charged, negatively charged and untreated membranes

Accurately weighed (W_d) membrane was wetted at ethanol, subsequently filtrated 1 litter of DI water for fully wetting. The sample was immersed in 0.1 N HCl solution for 24 h to exchange Na^+ into H^+ form. The sample was washed with DI water to remove any excess acid. After that, it was immersed in a 50 mL 3 N NaCl solution for 24 h. Exchanged amount of H^+ was titrated to the phenolphthalein endpoint with 0.1 N NaOH solution. The IEC value (meq/g) was then calculated using equation (2)

$$\text{IEC}\left(\frac{\text{meq}}{\text{g}}\right) = (V_{NaOH} \cdot N_{NaOH})/W_d \quad \text{..... (2)}$$

2.6.4. Determination of zeta potentials

The surface zeta potential of sample membranes was measured by electrophoretic light scattering spectrophotometer, ELS-Z1000 by Ostuka Electronics (Japan). Untreated PVDF membrane and charged membranes were prepared 1 × 3 cm^2, pre-wetted in ethanol. Then, samples were

measured in 10 mM NaCl solution that was pH controlled by solution of 0.1 M NaOH and 0.1 M HCl. Polystyrene latex particles for mobility monitoring particles of which surface charge is defined as 0 eV. The surface charge density of membranes was measured by zeta potential, which can be calculated using equation (3) [17].

$$\sigma = (8kTC_0\varepsilon)^{1/2}\sinh(ze\xi/2kT) \quad \text{..... (3)}$$

Value of *k* is the Boltzmann constant, *T* is the absolute temperature, C_0 is the bulk concentration, ε is the dielectric constant, z is the ion valence, e is the electron charge, and ξ is the zeta potential.

2.7. Evaluation of membrane performance

2.7.1. Measurement of membrane flux change due to protein fouling

To perform filtration experiments, the system was prepared as described in Figure 7. The tests were carried out using a 10 mL stirred ultrafiltration cell, Amicon model 8010 (U.S.A.) with a magnetic stirrer and an effective membrane area of 4.91 cm^2. A 1 gal stainless steel dispensing pressure vessel, Millipore (U.S.A.) was equipped with a pressure gauge and relief valve. The vessel was connected to the nitrogen gas cylinder and stirred cell to apply pressure to the cell. DI water permeability of the membrane was evaluated under the conditions below. The samples were pre-

wetted by ethanol. The reservoir was filled with DI water, and the filtration was pre-run at 1 bar for ~40 min until 1 L of DI water filtered to remove ethanol. The filtration cell was stirred at 200 rpm/min using a stirrer plate. To gain flux data, permeate weight was measured by an electronic balance CUW4200H, CAS corporation (Korea) that was linked to a computer for automated data gathering at wished time intervals. The flux J_w was calculated as equation (4).

$$J_W = permeate\ volume\ (L)/membrane\ area\ (m^2) \cdot time\ (h) \quad \ldots\ldots\ldots (4)$$

After that, the transmembrane pressure was set at 0.17 bar, pure water flux J_{w0} was collected. Then, protein solution (500 ppm) was prepared in phosphate buffer saline (PBS) with BSA or LYZ. It was prepared by dissolving salts (8 g of NaCl, 0.2 g of KCl, 1.44 g of Na_2HPO_4, and 0.24 g of KH_2PO_4) in 800 mL DI water. The pH was adjusted to 7.4 with 0.1 M HCl, subsequently added DI water to a total volume of 1 L. The resultant 150 mM PBS solution was diluted 2 times by added 1 L of DI water. The protein solution was filtered through the membrane for 1 h and the corresponding flux *J* was recorded during that time. After that, the samples were cleaned by back washing at 1 bar for 6 min (LYZ) and 1 min (BSA) in order to estimate the reversible fouling that can be recovered. The pure water flux J_{w1}. The evaluation of membrane performance was expressed in terms of the Normalized flux (equation 5), flux recovery ratio (equation 6).

$$\text{Normalized flux} = J/J_{w0} \quad \ldots\ldots\ldots\ldots\ldots\ldots\ldots\ldots\ldots\ldots\ldots\ldots\ldots\ldots\ldots\ldots (5)$$

$$\text{FRR} = J_{w1}/J_{w0} \quad \text{..... (6)}$$

As the value of FRR is higher, the antifouling property of the membranes is better. To study the antifouling properties in detail, total fouling (R_t), reversible fouling (R_r), irreversible fouling (R_{ir}), were calculated as follows:

$$R_t = [1 - J/J_{w1}] \cdot 100\% \quad \text{..... (7)}$$

$$R_r = [J_{w1}/J_{w0} - J/J_{w1}] \cdot 100\% \quad \text{..... (8)}$$

$$R_{ir} = [1 - J_{w1}/J_{w0}] \cdot 100\% \quad \text{..... (9)}$$

The value of R_t is the sum of R_r and R_{ir}. So smaller R_t means that the flux decline resistance property of the membranes is better.

2.7.2. Mixed protein separation (BSA-Hb)

Separating equipment was same as procedure 2.7.1. BSA-Hb (0.1 g/L: 0.1 g/L) protein buffer solution were prepared at isoelectric point of BSA (pH = 4.7) and Hb (pH = 6.8). Protein separation performance were enhanced at lower solution ionic strength, so acetate buffer solution and PBS buffer solution diluted 10 times, subsequently 0.1 M NaOH and 0.1 M HCl were added to adjust pH at 4.7 and 6.8. Preparation of PBS buffer solution was same as procedure 2.7.1. Acetate buffer solution was made by following processes. Acetic acid 0.2 M solution (11.55 mL in 100 mL of DI water) 20 mL plus sodium acetate 0.2 M solution (16.4 g of $C_2H_3O_2Na$ in 1 L of DI water) 30 mL and diluted to a total of 100 mL with DI water.

Prepared each buffer solution were filtrated with hydrophilic PVDF membrane filter (pore size 0.1 μm).

After each charged membranes were wetted by ethanol, they soaked in the desired BSA-Hb solution for overnight. The Amicon 8010 stirrer cell was filled with 18 mL protein solution. Protein separation was calculated by gain 4 mL sample of the filtrate protein solution after filtration of a minimum of 2 mL to certify equilibrium operation and to rinse out the dead volume downstream of the membrane. The detected sieving coefficient was calculated as follows:

$$S_0 = C_f / C_b \quad \text{..... (10)}$$

where, C_f and C_b are the protein concentration in the filtrate and bulk solutions. To express the protein separation performance of charged membranes for the BSA-Hb solution, the separation value is defined as follows:

$$\varphi_{BSA/Hb} = S_{0,BSA} / S_{0,Hb} \quad \text{..... (11)}$$

where, $S_{0,BSA}$ and $S_{0,Hb}$ is the sieving coefficient of BSA, and Hb.

The protein concentration were detected by and ultraviolet visible spectrophotometer (Uv-Vis) UV-1650PC by Shimadzu (Japan) with standard solution. The following procedures are performed for preparation of standard solution.

Solution A: Dissolve 40 mg of BSA or Hb in a 40 mL buffer at pH 4.7 or 6.8 (protein content: 1000 ppm)

Solution B: Dilute 10.0 mL of solution A with 10.0 mL of buffer (protein content: 500 ppm)

Solution C: Dilute 10.0 mL of solution A with 15.0 mL of buffer (protein content: 200 ppm)

Solution D: Dilute 15.0 mL of solution A with 15.0 mL of buffer (protein content: 100 ppm)

Solution E: Dilute 15.0 mL of solution A with 5.0 mL of buffer (protein content: 75 ppm)

Solution F: Dilute 10.0 mL of solution A with 5.0 mL of buffer (protein content: 50 ppm)

Solution G: Dilute 5.0 mL of solution A with 5.0 mL of buffer (protein content: 25 ppm)

Solution H: Dilute 3.33 mL of solution A with 3.33 mL of buffer (protein content: 12.5 ppm)

Each protein solution mixed 1:1 and detected by Uv-Vis, used to draw standard curve. The maximum absorbance of the BSA standard solution exhibits at 280 nm, whereas the maximum absorbance of Hb standard solution displays two points at 280 nm and 408 nm. Hence, the Hb concentration in the BSA-Hb mixture was determined from the absorbance at 408 nm, used to calculate Hb absorbance at 280 nm. The absorbance of BSA at 280 nm was gained by subtracting the Hb contribution at this position from the total absorbance at 280 nm [33, 34].

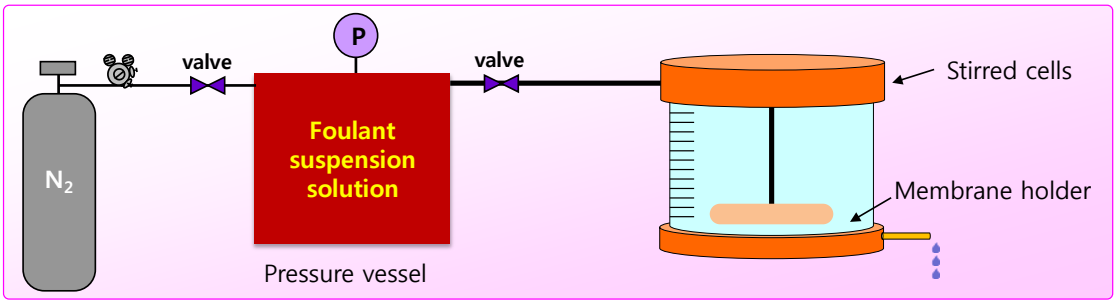

Figure 8. Schematic illustration: evaluation of membrane performance

3. Results and Discussion

3.1 Characteristics of NH_2-HPG, NH_2-PHPG, NH_2-NHPG

3.1.1. FT-IR and ^{1}H NMR

Synthesis of hyperbranched polyglycerol

The polymerization of charged HPG with one relatively high reactive amine group is done in order to manufacture the charged PVDF membrane that was attached one linker to one charged HPG in a grafting-to approach (Figure 1).

First, use tris(hydroxymethyl)aminomethane (THAM) as initiator-core. In order to protect amino functionality during the basic conditions present in the anionic polymerization and charge inducing process, put a benzyl bromide to occur SN2 reaction (Figure 2). ^{1}H NMR spectroscopy (Figure 10) has been used to determine the synthesized N,N-dibenzyl tris(hydroxymethyl) Aminomethane (Bz_2-THAM) by comparing the integration of benzyl protective groups (7.28-7.02 ppm) and other proton peaks (Table 1). Integral ratio of experimental peaks agreed reasonable with theoretical peaks of them.

Table 1. Integral ratio of Bz_2THAM by ^{1}H NMR

Position	Integral ratio	
	theoretical	experimental
3	3.00	3.04
1	6.00	6.03
4, 5, 6	10.00	10.14
2	4	4.05

The hydroxyl groups of Bz_2-THAM were partly deprotonated using cesium hydroxide for the ring opening multi-branching polymerization (ROMBP) of glycidol, which was added slowly in sample solution at 100 ℃. As presented in ^{1}H NMR spectra (Figure 10), benzyl protective groups and the polyether backbone were clearly distinguished. Comparing the integral ratio of the ether groups and the benzyl groups in Bz_2-HPG, determined the degree of polymerization (DP_n) and absolute number-average molecular weight (M_n). Table 2 shows the DP_n and M_n of the HPG. Both experimental values 21.1 and 1864.5 g/mol are coincide with target value 21 and 1864.5 g/mol. This experimental result are more resembled with target value than conventionally polymerized HPG that used initiator as TMP (1,1,1-trimethylol propane) [35]. It is because benzyl protective groups increase the solubility of initiator that facilitates higher degrees of deprotonation, which prevent side-reaction (e.g. self-initiation of glycidol) [27].

Next, using catalyst Palladium on charcoal (Pd/C) and acetic acid remove benzyl protective groups by hydrogenolysis (Figure 6). In this research, hydrogen pressure, reaction temperature, and reaction time is reduced than advanced research [27]. Since, acid additive such as acetic acid was effective for debenzylation, because hydrogenation of polarized σ bond is more suitable than nonpolarized bonds [28, 36]. As clearly seen in Figure 10, comparison of Bz_2-HPG and NH_2-HPG, the benzyl peak (7.47−7.16 ppm) of NH_2-HPG disappeared. Figure 9 shows IR spectroscopy of NH_2-

HPG that characterize for –OH at 3650-3200 cm^{-1}, sp^3 C-H stretch at 3000-2850 cm^{-1} and C-O stretch at 1100-1000 cm^{-1}.

Functionalization of hyperbranched polyglycerol

HPG was positively charged due to electrophilic ring opening reaction with activated hydroxyl group of Bz_2-HPG and glycidyl trimethylammonium chloride (GTA) as additive monomer [29]. Figure 9 shows the Fourier transform infrared spectroscopy (FT-IR), the C-H bend 1480 cm^{-1} of quaternary group at GTA and cationic charged HPG. It was also seen in ^{1}H NMR spectroscopy (Figure 10). Ether bond was confirmed at 4.35 ppm (peak e), which was formed by reaction with the basic conditions present in hydroxyl groups of NH_2-PHPG and epoxy ring of GTA. In addition, signal of methyl protons adjacent to quaternary ammonium group was appeared at 3.16 ppm. The degree of substitution (DS) was determined by calculating the integration ratio of the benzyl peak 4-6 and ether peak e. Table 2 shows reaction condition and DS that indicates almost 100% reaction of hydroxyl groups of HPG and GTA, the average number of quaternary ammoniums per polymer is 21. Deprotection of positively charged HPG was also, well defined at Figure 10.

Negatively charged HPG was acquired by sulfonation of Bz_2-HPG using the sulfur trioxide pyridine complex (STPC) [30]. The IR spectra of both STPC and NH_2-NHPG showed the S=O stretch 1259 $cm^{-}1$ and C-O-S stretch 805 $cm^{-}1$ (Figure 9). ^{1}H NMR spectra showed ether bond g and f

(4.24-4.75 ppm) developed by reaction with the end groups of Bz_2-NHPG and sulfur trioxide of STPC compound. In addition, integral ratio of benzyl group and ether peak g, f peak indicated degree of sulfonation (DS) of the hydroxyl groups in NH_2-NHPG, approximately 67% (Table 2). To deprotect benzyl group in Bz_2-NHPG, it was dissolved in mixture of 1:1 ethanol and DI water because ionic characteristic of sample makes it hard to dissolve in pure ethanol. Linda Nikoshvili et al. [37] said that activity of catalyst in ethanol and DI water solution is lower than pure ethanol. For that reason, reaction that supplies hydrogen to Bz2-NHPG progressed longer time than neutral and positively charged Bz_2-HPG. After 4 days of hydrogenolysis process, benzyl group of negatively charged HPG was disappeared clearly (Figure 10).

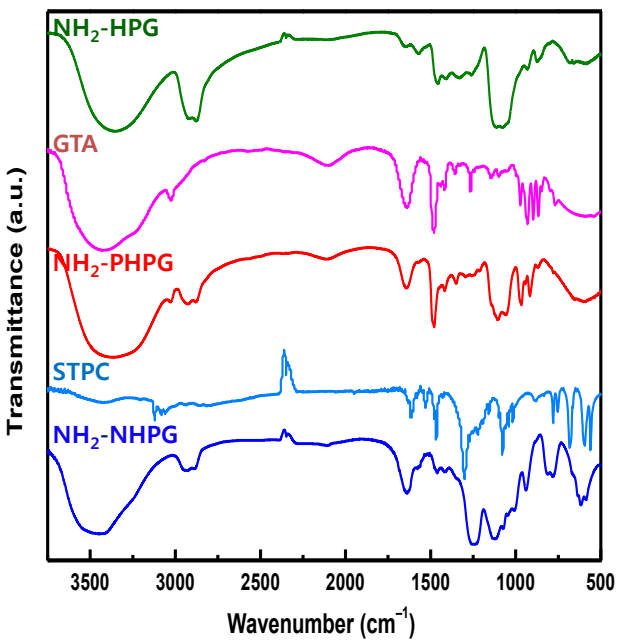

<Stretching and bending vibration>

sp^3 C–H stretch (3000–2850 cm^{-1})
O–H stretch (3650–3200 cm^{-1})
C–O stretch (1100–1000 cm^{-1})
C–H bend of N^+(1480 cm^{-1})
Ring stretch (930–910, 890–820 cm^{-1})
C–H and epoxy ether vibration
(3024, 1260 cm^{-1})
C=C stretch (1691 cm^{-1})
C=N stretch (1677 cm^{-1})
S=O stretch (1259 cm^{-1})
C-O-S stretch (805 cm^{-1})

Figure 9. FT-IR spectrum of NH_2-HPG, GTA, NH_2-PHPG, STPC, NH_2-NHPG

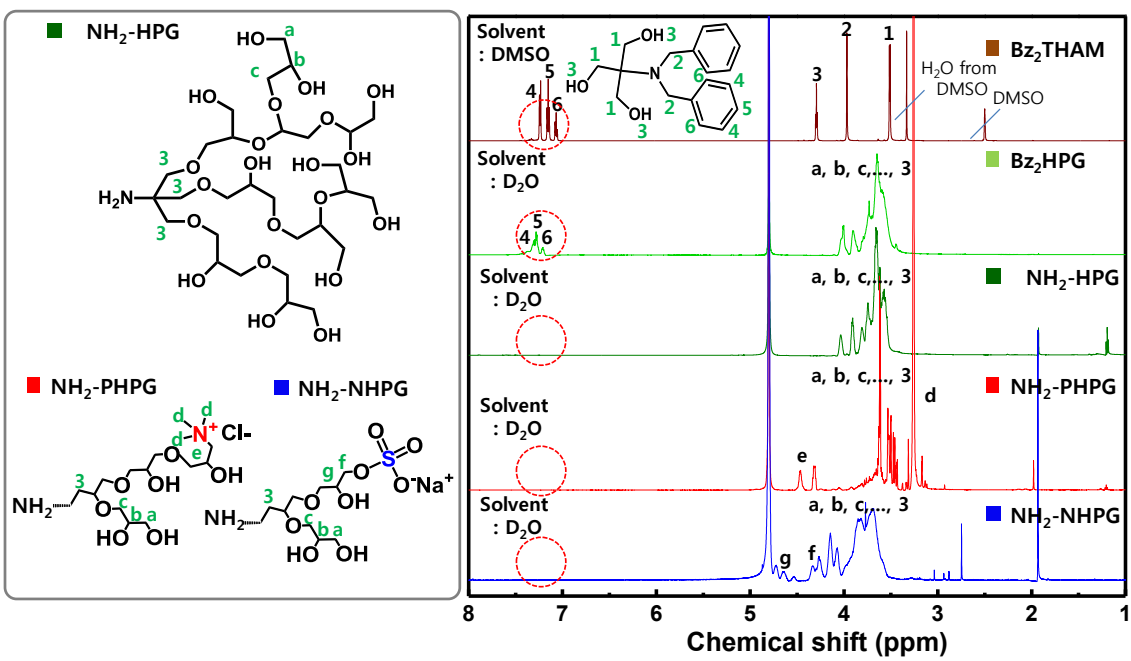

Figure 10. ^{1}H-NMR spectra of Bz_2THAM, Bz_2-HPG, NH_2-HPG, NH_2-PHPG, NH_2-NHPG

Table 2. Interpretation of ^{1}H NMR spectra of NH_2-HPG, positively charged PHPG, and negatively charged NHPG

***DPn:** degree of polymerization
***DS:** degree of substitution

Sample code	End group	OH : additive ratio	*DP_n or *DS
NH_2-HPG	3	1 : 21 (glycidol)	21.1
Bz_2-PHPG	24.1	1 : 1.2 (GTA)	0.996
Bz_2-NHPG	24.1	1 : 1 (STPC)	0.67

3.2. Characteristics of membrane

3.2.1. ATR-IR and XPS

In order to connect the HPG and charged HPG on PVDF membrane surface, plasma treatment was performed to introduce functional groups due to chemical resistance of neat-PVDF membrane (Figure 1). To link functional groups of plasma treated PVDF membrane and charged HPG, use 1,4-phenylen diisocyanate (PDC) as linker agent. Each isocyanate groups of PDC react with membrane and one focal amino group of HPG and charged HPG. Isocyanate allow selective chemical reaction of amine groups in the presence of multiple –OH groups of H_2O, ethanol (solvent) and end groups of HPG because degree of deferent relative reaction rate of Primary aliphatic amine (100,000), Primary hydroxyl group (100), and water (100) is large.

The ATR-IR spectra of HPG and charged HPG attached PVDF membranes are shown in Figure 11. From ATR-IR spectrum of PVDF-HPG, PVDF-PHPG, and PVDF-NHPG, it shows that the band at 3600-3200 cm^{-1} is corresponded to the stretching vibration of –OH and –NH groups. The absorption peaks at 2273 cm^{-1}, 1700-1748 cm^{-1}, 1637 cm^{-1} and 1555 cm^{-1} are reacted and unreacted isocyanate groups of PDC linker peaks, which are attributed to the –NCO, -C=O, -N-H deformation vibration, and N-H amide Ⅱ bend [38, 39].

XPS analysis on membranes was done to determine chemical compositions and chemical bonding of HPG and charged HPG attached PVDF membrane more specifically. Figure 12, 13, and 14 show XPS spectra for the surface of the neat-PVDF membrane and the membranes produced by reaction with the linking agent PDC, neutral HPG, positively charged HPG, and negatively charged HPG. In the case of neat-PVDF membrane, the C 1s spectra can be fitted with two main components peak, with binding energies (eV) at 284.5 eV for the CH or C-C species and 289.03 eV for the CF_2 species [10, 15, 40, 41]. Linker attached PVDF membrane obtained C 1s spectra peak with binding energy at 287.59 eV for the C=O species and N 1s spectra peak with binding energy at 399.0 eV for the N-H species that was contained at unreacted isocyanate of PDC linker and reacted one. HPG and charged HPG linked membranes obtained C1s spectra peak with binding energy at 285.72-285.97 eV for C-O species of linked HPG and charged HPG. The spectra of PVDF-PHPG in Figure 13 were obtained at energies near the neutral amine and positively charged nitrogen (N^+) species (binding energy of approximately 399.28 eV and 402.35 eV) while those in Figure 14 are focused on the sulfur peak (binding energy at 168.85 eV). These result revealed that the quaternary ammonium group possesses positively charged PHPG and the sulfur trioxide group possesses negatively charged NHPG were well connected at the charged membranes.

The area under the C, O, N, and S peaks determined the atomic

composition of the different each membranes (Table 3). The atomic and mass concentration percent (Conc.%) of nitrogen and sulfur are both absent, oxygen content are less than 2% in the XPS data at neat-PVDF membrane. However, nitrogen is clearly visible and oxygen concentration is more than 10% for the all treated membranes. The negatively charge-modified PVDF membrane (PVDF-NHPG) is the only sample that has sulfur conc.%. So surface composition data of XPS also exposed that polymer such as linker, HPG, PHPG, and NHPG are fairly introduced in treated sample membranes.

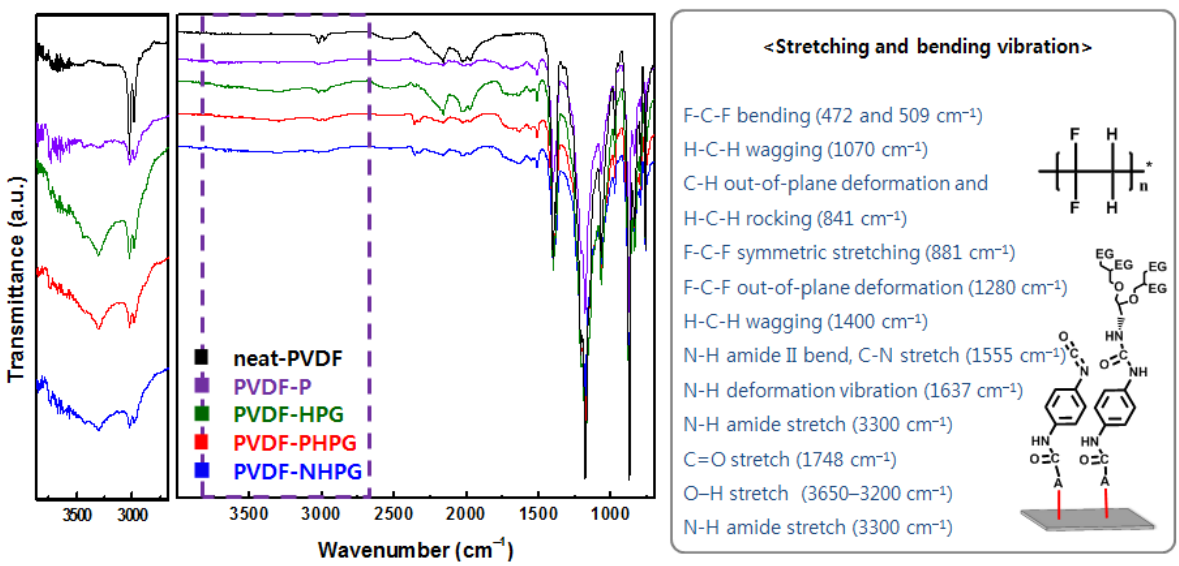

Figure 11. ATR-FTIR Spectra of NH_2HPG attached PVDF membrane

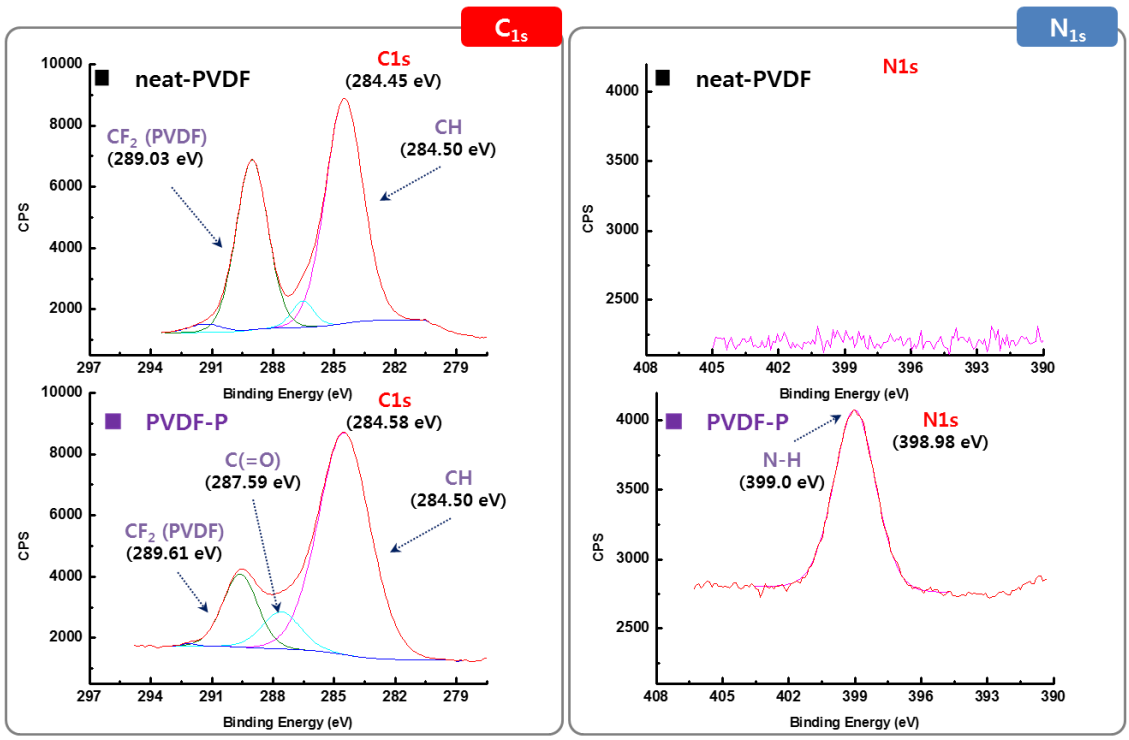

Figure 12. XPS spectra of neat-PVDF membrane and PDC linker attached PVDF-P membrane

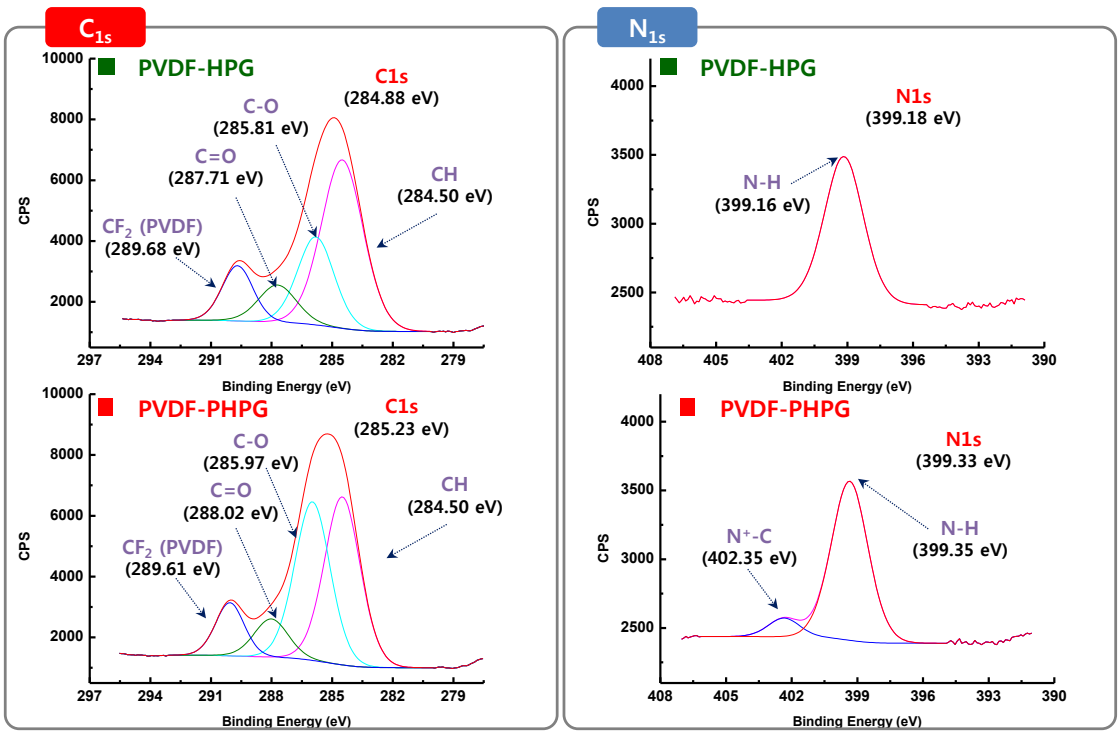

Figure 13. XPS Spectra of NH_2HPG, NH_2PHPG attached PVDF membrane

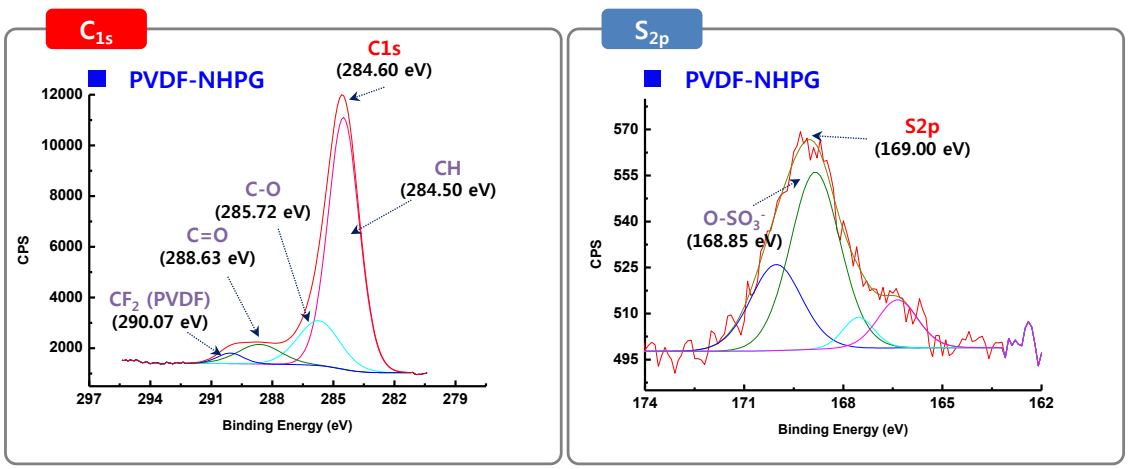

Figure 14. XPS Spectra of NH_2NHPG attached PVDF membrane

Table 3. Atomic conc.% of surface composition of charge-modified membrane

sample / peak	neat-PVDF	PVDF-HPG	PVDF-PHPG	PVDF-NHPG
C_{1s}	48.73	52.55	64.42	71.07
N_{1s}	0	3.26	3.56	4.72
O_{1s}	1.74	18.13	14.96	12.52
F_{1s}	49.53	26.06	17.06	11.44
S_{2p}	0	0	0	0.24

3.2.2. Surface morphology and water contact angle of membrane

To determine whether the atmospheric-pressure plasma treatment and polymer (HPG and charged HPG) attach process altered the physical morphologies of the membrane, FE-SEM images were obtained for the neat and charge-modified PVDF membrane (Figure 15). The surface of neat-PVDF membrane was seen sharp and tough pore structures, but surface of HPG and charged HPG attached membrane has somewhat smoother pore structures that was slightly altered than neat one. Penetration of the atmospheric pressure plasma through the pores in the PVDF membrane transfer heat. In addition, etching effect also occurred, which makes pore structure of charge-modified membrane smoother. Unlike FE-SEM images of membrane, which was grafting treated with monomers, pores of HPG and charged HPG attached membranes has not bumpy and adversely narrow structure than untreated membranes [42]. These treatments did not altered surface structure of membrane significantly.

It was characterized by the water contact angle value (CA) that the change in the hydrophilic property of the membrane surfaces after HPG and charged HPG attachment (Table 4). The surface of neat-PVDF membrane had a water CA value of ~136.2°, demonstrating a severe hydrophobic nature. The surface of charge-modified membranes had smaller CA approximately 30-50°, representing increase of hydrophilic nature than neat one. It is found that negatively charged membrane (PVDF-NHPG) has larger CA than neutral and

positively charged membrane (PVDF-HPG, PVDF-PHPG). Negatively charged HPG gained solid state (ionic state), different with gel formed HPG and positively charged HPG. Also after addition of negatively charged sulfur trioxide at end group of hydroxyl group, they were disappeared unlike HPG and PHPG. Therefore, during surface modification process, plasma treated PVDF membrane was dipped in NHPG solution base of DI water, which could not wet PVDF membrane contrary to ethanol. Difference of modification process and less hydroxyl group of HPG, PVDF-NHPG sample might linked charged HPG lesser than PVDF-HPG and PVDF-PHPG. It can also be seen at Figure 16. Nevertheless, the CA measurements indicate the treated PVDF membranes are hydrophilic compared to the neat-PVDF membrane.

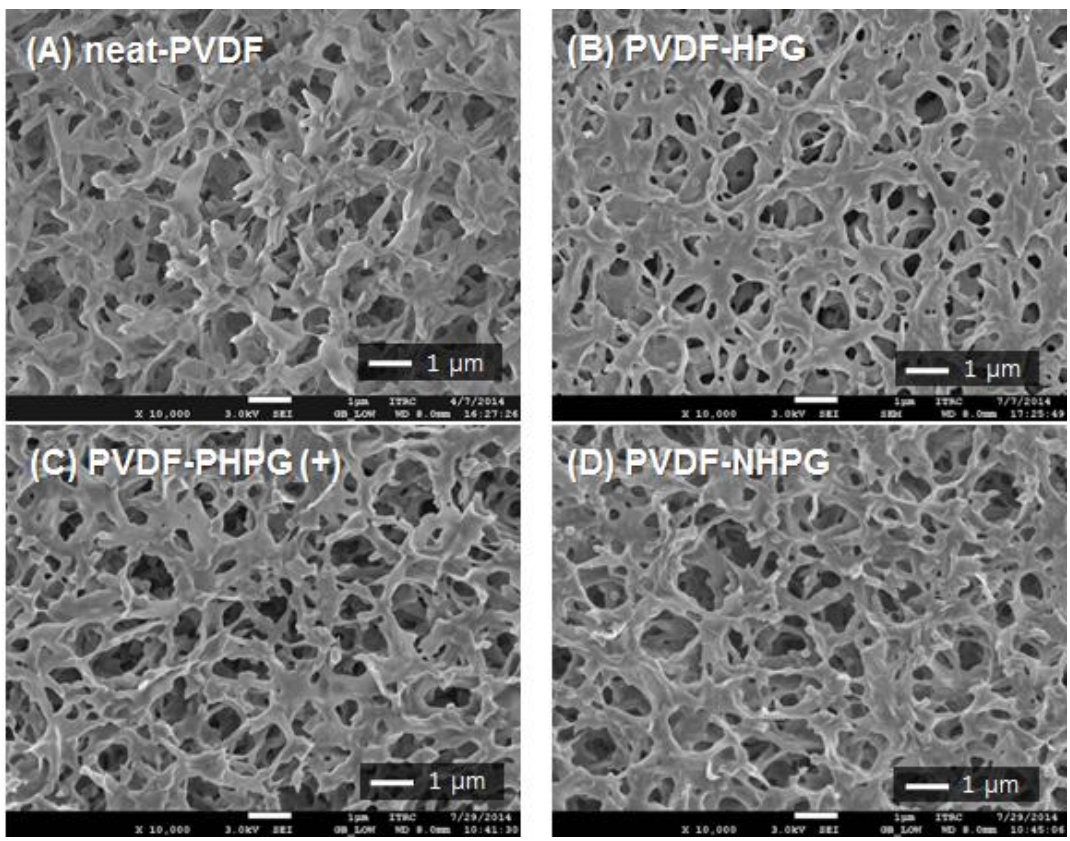

Figure 15. FE-SEM images of the neat-PVDF membrane (A), neutral charge-modified PVDF-HPG membrane (B), positively charged PVDF-PHPG membrane (C), and negatively charged PVDF-NHPG membrane

Table 4. Water contact angle (CA) of the neat-PVDF membrane and charge-modified membranes

Sample code	Water contact angle	Image
neat-PVDF	136.2° ± 5.2	
PVDF-HPG	81.7° ± 2.5	
PVDF-PHPG	80.7° ± 6.9	
PVDF-NHPG	110.5° ± 2.0	

3.2.3. Charge Property of membrane surface (IEC and Zeta potential)

The content of sulfonic acid groups of the negatively charged PVDF-NHPG membrane and quaternary ammonium groups of the positively charged PVDF-PHPG membrane was measured through IEC. The IEC value of the neat-PVDF membrane, PVDF-HPG membrane, and charged two membranes with degree of substitution are shown in Figure 16. IEC value of the charged membranes was higher than that of the neat-PVDF membrane and PVDF-HPG membrane. These data shows charged membranes were endowed charge characteristics, that means positively charged HPG and negatively charged HPG were linked on PVDF-NHPG membrane and PVDF-PHPG membrane. However, charge modification was done on the very top of the surface layer only. There for, IEC value of charged membranes was not that much. From the Figure 16, IEC value of positively charged PVDF-PHPG was higher than PVDF-NHPG. It means degree of substitution value of positively charged PVDF-PHPG membrane were higher than negatively charged PVDF-NHPG membrane. Tendency of this result was same as CA value.

The IEC value revealed that charge-modified PVDF membrane included charged matters. To measure more clear data of charge-modified membranes charge property, zeta potential measurement were shown in Figure 17. It has a substantial influence on the fouling performance on membrane filtration process

that the membrane has surface charge property [17]. During filtration process, attachment and detachment of foulants can be controlled by the electrostatic interaction between surface of the charged membrane and charged foulants. Charged matter makes formation of electric double layer, composed of a fixed layer and a diffuse layer. The border between immobilized layer and diffuse layer called shear plane. It is called the zeta potential (ξ) that caused by ions stream on the shear plane. For pH values from around 3-10, neat-PVDF membrane firstly had positive ξ value around pH 3, passed through an isoelectric point (PI) at ~pH 3.7 and is negatively charged above those pH value. This zeta potential value was similar to advanced research [43]. The Positively charged PVDF-PHPG membrane and neutral PVDF-HPG membrane presented positive zeta potentials for all detected pH values (pH 3-10). The positively charged PVDF-PHPG membrane has a higher zeta potential value than PVDF-HPG, which has positive but almost neutral zeta potential value. The negatively charged PVDF-NHPG has negative zeta potential in the whole pH region, having lower zeta potential than neat-PVDF membrane. The linked HPG and charged HPG provide different electrical properties on the membranes, which can have an effect on the fouling performance during filtration that using charged substances.

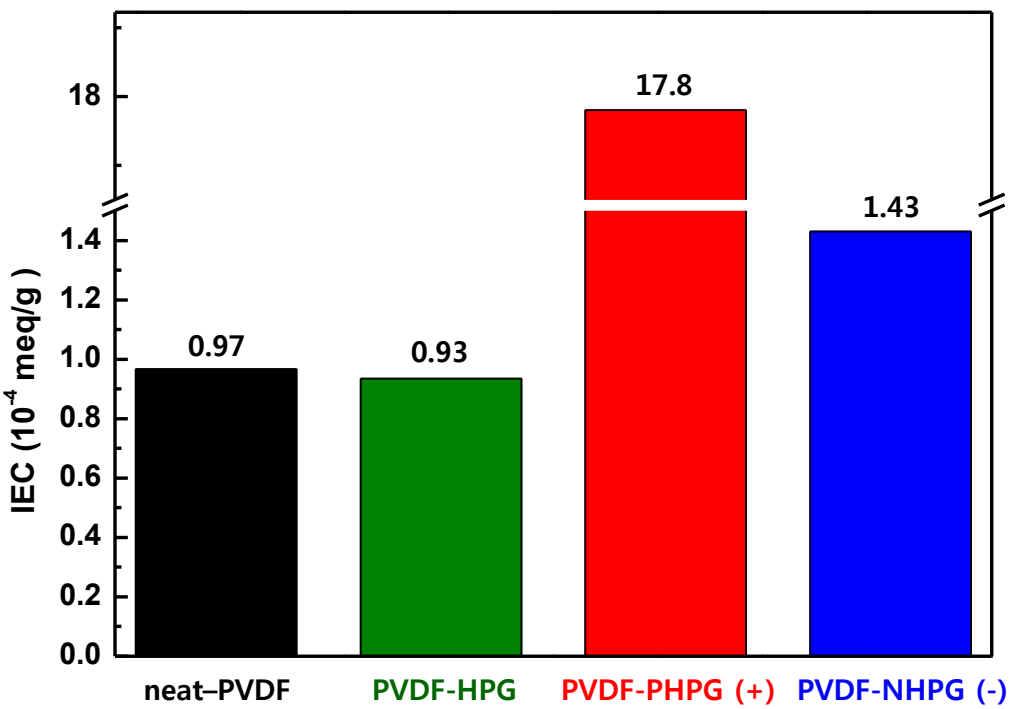

Figure 16. Ion exchange capacity (IEC) of the neat-PVDF membrane and charge-modified membranes

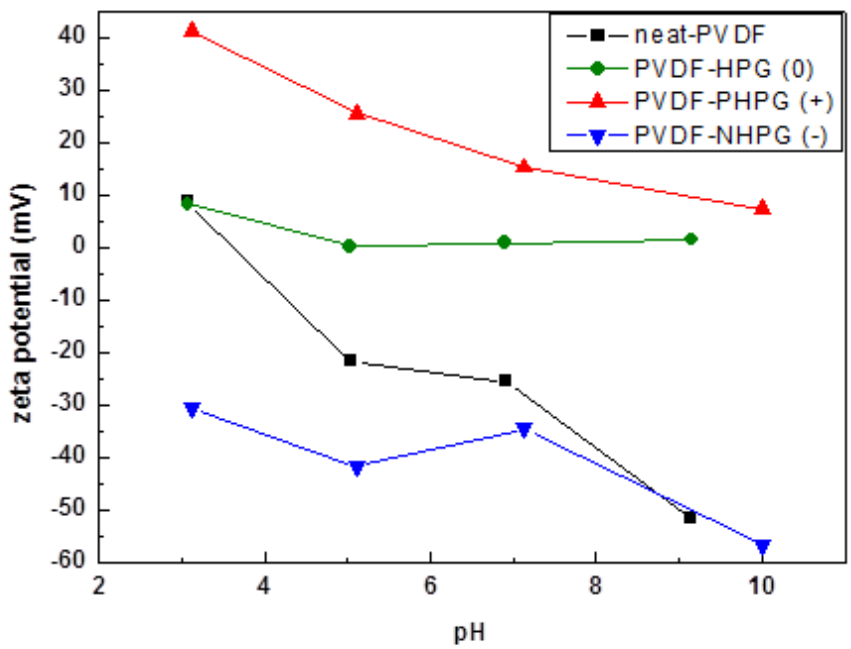

Figure 17. Zeta potential of neat-PVDF, PVDF-HPG, PVDF-PHPG, and PVDF-NHPG in 10 mM NaCl solution.

3.3. Protein ultrafiltration

Using Lyz and BSA as positively and negatively charged foulants, fouling behaviors at neat, neutral, and charged PVDF membranes were conducted. At pH 7.4, adapted by PBS, Lyz was positively charged ($\xi \sim +3.5$ mV) and BSA was negatively charged ($\xi \sim -22.3$ mV) [42]. Table 5 shows the DI water penetration value of neat and altered membranes. Permeate flux values were similar due to usage of standard sized purchased PVDF membrane, ethanol wetting before permeate test, one-shot reaction of one to one surface grafting reaction with linker and charged HPG, different from monomer grafting method. Nevertheless, the surface property of charge-modified membrane had a substantial influence on the filtrate flux of the protein solutions. Figure 18-21 shows Lyz and BSA fouling performances during the permeate tests using neat and charge-modified PVDF membranes.

For Lyz solutions (Figure 18), the normalized flux declined with time for the samples. Such trend was caused by the increase of the adsorbed Lyz on the surface of membranes during filtration test. The normalized flux of neat PVDF membrane declined significantly with times. In contrast, the filtrate flux declined slower for all charge-modified membranes than neat-PVDF membrane. Due to the surface modification of PVDF membrane with HPG and charged HPG, hydrophilic property endowed, achieved high fouling resistance. Likewise, at pH 7.4, surface zeta potential of neat-PVDF

was negative value so electrostatic interaction between Lyz and membrane surface accelerate Lyz adsorption, which decreased normalized flux. Among normalized flux of treated samples, this value of positively charged PVDF-PHPG membrane samples was highest. The majority decreasing rates of the normalized fluxed through the neutral charged PVDF-HPG was intermediate level and that value of negatively charged PVDF-NHPG was lowest. These trends also can be seen at Figure 19. During 3 cycles of permeate test, the irreversible fouling value was highest at neat-PVDF and these values decreased PVDF-NHPG, PVDF-HPG, PVDF-PHPG in this order except cycle 2. Mean reversible fouling was highest at positively charged PVDF-PHPG. It means that positively charged surfaces would repulse the positively charged Lyz, so they reduce adsorption of Lyz (low irreversible fouling) and increase detachment of Lyz during back washing (high reversible fouling).

For BSA solutions, opposite trend of the normalized flux decrease was seen except for neat-PVDF membrane (Figure 20). At pH 7.4, the zeta potential value of neat-PVDF and negatively charged PVDF-NHPG was negative, so electrostatic repulsion between BSA and membrane surface was occurred. As a result, normalized flux value was higher at negatively charged BSA solution than positively charged Lyz solution. The neat-PVDF membrane has hydrophilic property and lower zeta potential value than those of neat-PVDF membrane. Figure 21 shows reversible fouling and irreversible fouling. During 3 cycles, mean reversible fouling was highest at

negatively charged PVDF-NHPG, negatively charged surface and BSA would repel each other, so total fouling was smallest, backwashing efficiency was highest, and irreversible fouling was lowest. The positively charged PVDF membranes surfaces attract negatively charged BSA, so irreversible fouling was highest at cycle 1. The fouling and decrease of normalized flux was intermediate at neutral charged PVDF-HPG. However, CA (hydrophilic property) of PVDF-HPG and PVDF-PHPG was lower than CA of neat-PVDF, so fouling degree was more stable at PVDF-HPG and PVDF-PHPG. After 3rd cycles of lysozyme solution filtration, order of flux recovery ratio (FRR) were; positively charged PVDF-PHPG membrane (57%) > neutral charged PVDF-HPG membrane (49.1%) > negatively charged PVDF-NHPG membrane (41.8%) > neat-PVDF membrane (31.4%). At bovine serum albumin solution filtration, FRR were; negatively charged PVDF-NHPG membrane (83.3%) > neutral charged PVDF-HPG membrane (75.9%) > positively charged PVDF- neat-PVDF membrane (70.1%) > PHPG membrane (67.3%). Overall, the increase in hydrophilic property and the reduced tendency for ion adsorption by the grafted charged HPG on PVDF membrane surface improved the protein resistant character because hydrophilic property and electrostatic interaction driving force for adsorption can be reduced. Thus, membrane surface grafting modification with charged HPG makes eco-friendly membrane as application to various wastewater (e.g. positively charged matter rich wastewater, made by soda

lime glass manufacture process or negatively charged humic acid rich wastewater) applications.

Table 5. Water flux of the neat-PVDF membrane and the charge-modified membranes at 1 atm

Sample code	neat-PVDF	PVDF-HPG	PVDF-PHPG	PVDF-NHPG
Flux (L/m^2h)	2635.0	2883.8	2629.3	2534.8

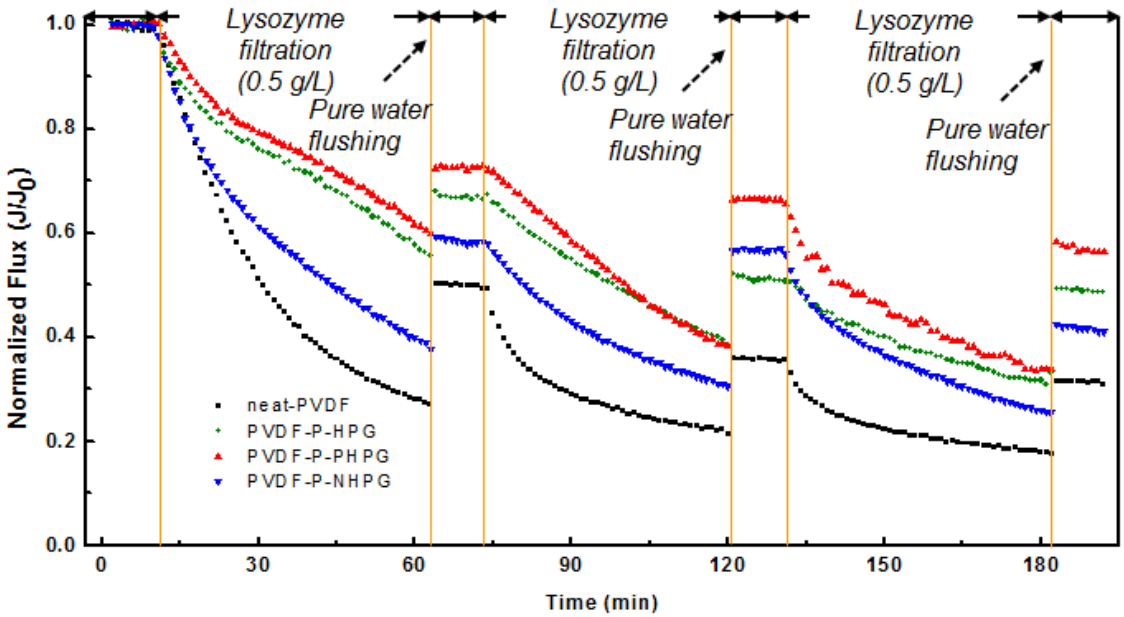

Figure 18. Filtration test of neat-PVDF membrane and the charge-modified membranes using lysozyme as positively charged foulants

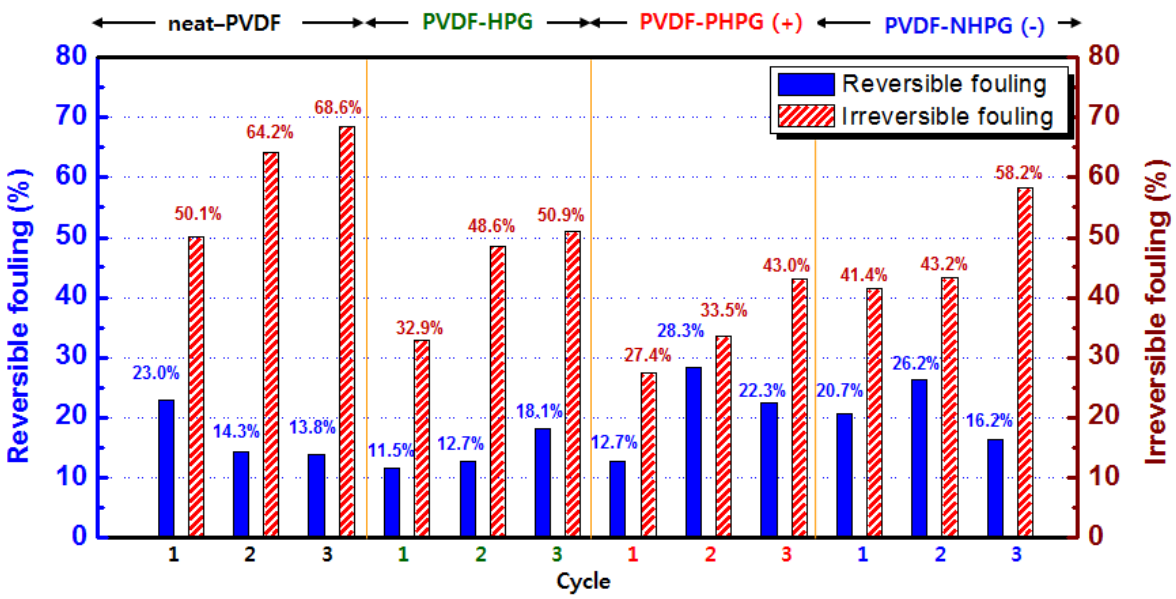

Figure 19. Reversible fouling and irreversible fouling of neat-PVDF membrane and the charge-modified membranes during filtration test using lysozyme as positively charged foulants

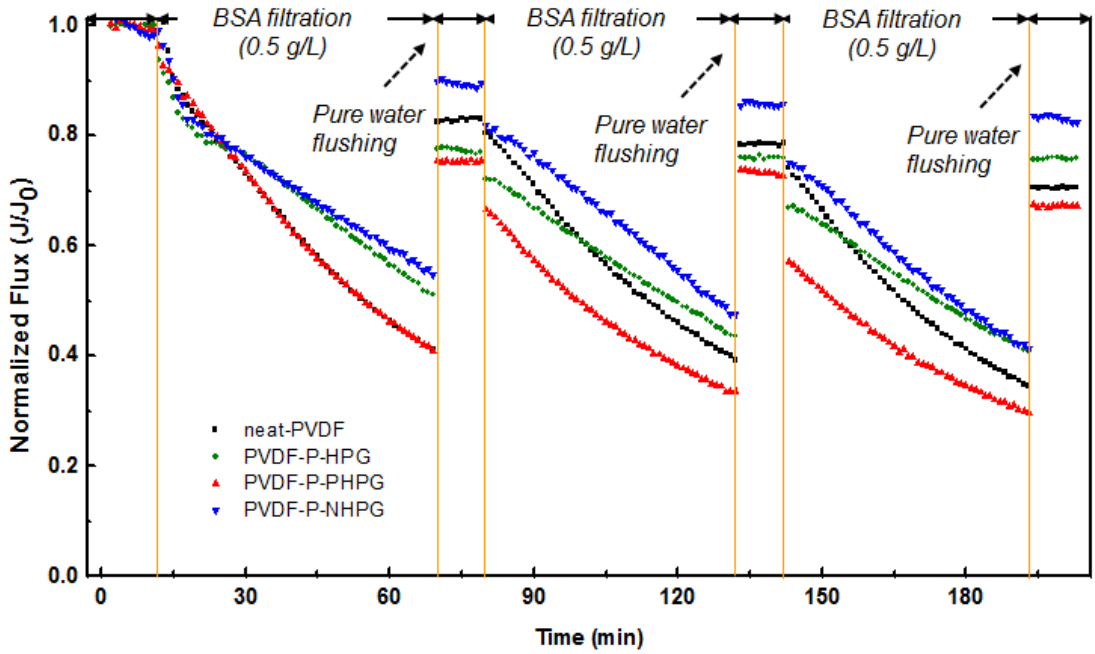

Figure 20. Filtration test of neat-PVDF membrane and the charge-modified membranes using bovine serum albumin as negatively charged foulants

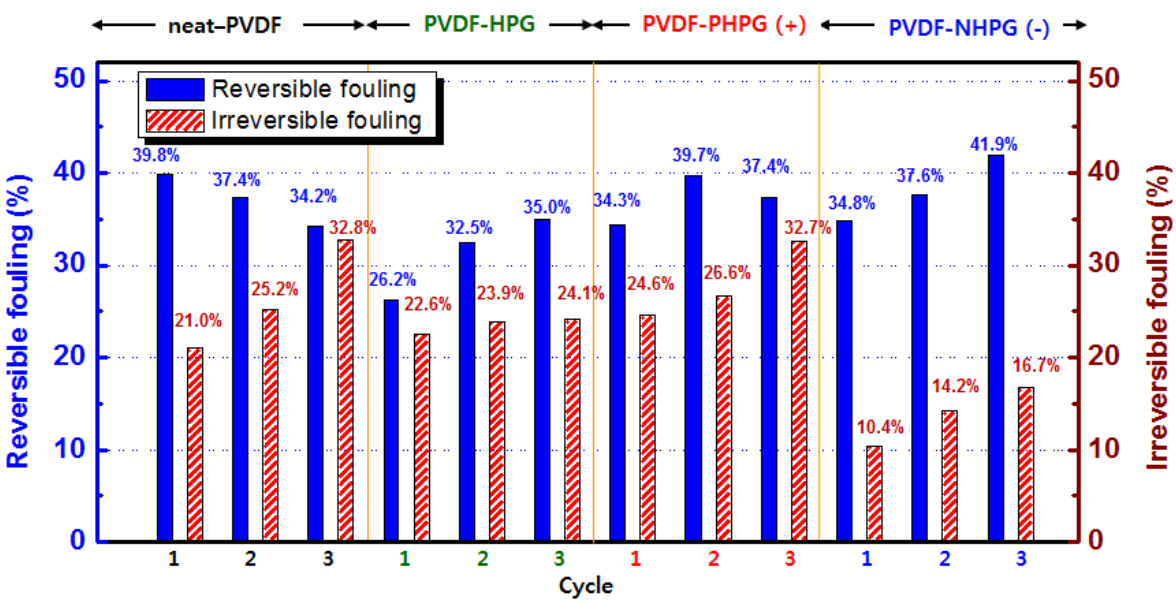

Figure 21. Reversible fouling and irreversible fouling of neat-PVDF membrane and the charge-modified membranes during filtration test using bovine serum albumin as positively charged foulants

To measure membranes surface charge effect during protein separation, we used two similar-sized proteins BSA and Hb in bovine blood. They have nearly identical molecular weights (Hb 64.5 kDa, BSA 66.5 kDa), but has different isoelectric point (PI of BSA = 4.7, PI of Hb = 6.8). The PI of protein has a key role in separation. When the pH of a protein solution is equal to the PI of a protein, proteins surface charge is neutral. When a pH is lower than PI, the protein is positively charged; at a pH is higher than PI, the protein is negatively charged [44]. The number of research said that high degree of selectivity obtained under pH of buffer solution is equal to the proteins PI value [45-49]. Therefore, at pH 4.7, BSA selectivity was high due to the strong electrostatic exclusion of the positively charged Hb molecules from the membrane pores, with the BSA permeation remaining relatively high due to the absence of substantial net charge on the neutral BSA at this pH value. At pH 6.8, Hb selectivity was high vice versa. As a result, to determine two proteins separation performance using charged PVDF membrane at each PI value, filtration process of protein solution was performed at pH 4.7 and pH 6.8.

Figure 22 shows that at pH 4.7, sieving coefficient S_0 of the BSA (permeate ratio) was a little bit higher than S_0 at pH 6.8. Likewise, S_0 of Hb at pH 6.8 was a little bit higher than S_0 at pH 4.8. Thus, BSA selectivity was higher at pH 4.7 and Hb selectivity was higher at pH 6.8. However, membranes pore size is ~10 times larger than proteins, so the protein separation effect was insignificant by titration of pH value to PI value of protein.

Advanced research said that charged membranes has greater protein separation ability by electrostatic repulsion or adsorption [22, 44, 45, 47, 48]. At pH 4.7, positively charged Hb was effectively retained by the negatively charged PVDF-NHPG by electrostatic interaction, so, the S_0 value of Hb at PVDF-NHPG was approximately 0.36 below at Figure 22. The S_0 values of BSA at pH 4.7 by each charge-modified membranes were comparable. As a result, BSA selectivity was highest at pH 4.7 by negatively charged PVDF-NHPG. At pH 6.8, negatively charged BSA was successfully adsorbed by the positively charged PVDF-PHPG membrane, while neutral Hb easily filtrated through the membrane. For that reason, Hb selectivity was highest by positively charged PVDF-PHPG at this condition. The pore size of purchased PVDF membrane was standardized to 100 nm. The size of the protein Hb is $6.5\times5.5\times5$ nm^3, and its shape is sphere-like, while the size of BSA is $14\times4\times4$ nm^3, and it resembles a globular ellipsoid [50]. The pore size of membrane is too large to use proteins separation processes electrostatic repulsion effect between surface of charged membrane and charged proteins was not observed. Nevertheless, protein separation effect by electrostatic interaction using charged membrane was seen. These results are suggesting that if additional experiments were conducted by the charge-modified membrane, which has appropriate pore size to protein separations, these membranes can be used for efficient charged particle-separation application.

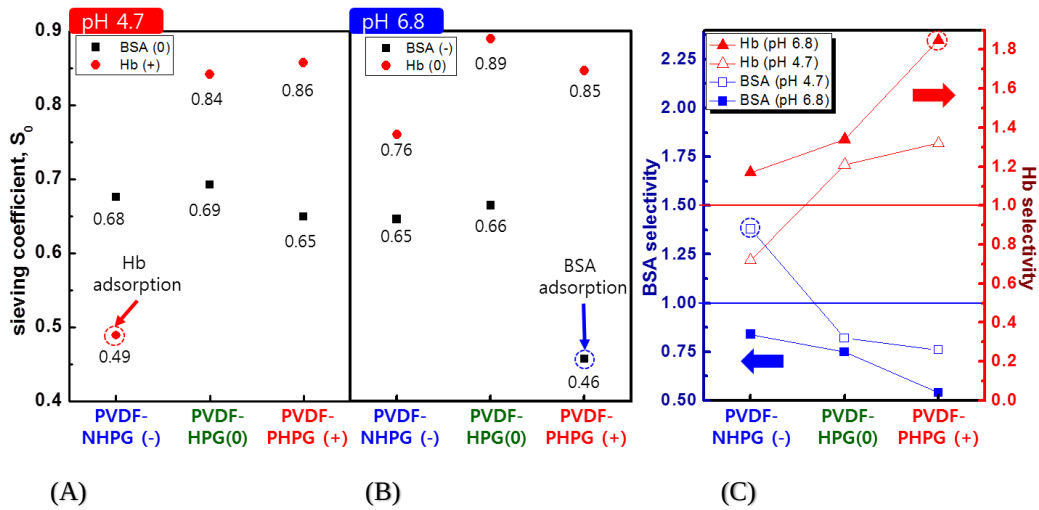

(A) (B) (C)

Figure 22. Sieving coefficient of PVDF-HPG, PVDF-PHPG, and PVDF-NHPG at pH 4.7 (A) and sieving coefficient of PVDF-HPG, PVDF-PHPG, and PVDF-NHPG at pH 6.8 PBS (B) and protein selectivity of PVDF-HPG, PVDF-PHPG, and PVDF-NHPG at pH 4.3 and pH 6.8

4. Conclusions

We developed various charge-modified membrane to improve anti-fouling efficiency against numerous charged contaminants. Initially, a hydrophilic hyperbranched polyglycerol, possessing one focal amine group (NH_2-HPG) was prepared from the ring opening multi-branching polymerization of glycidol, subsequently positively charged GTA or negatively charged STPC was used to modify them. Charged PVDF membranes were fabricated by reaction with linking agent, attached on plasma treated PVDF membrane and charged HPG. FT-IR and ^{1}H-NMR study confirmed the successful polymerization of NH_2-HPG and charge modifying degree of PHPG (100%) and NHPG (67%). ATR-IR and XPS spectra confirmed attachment of neutral and charged HPG on surface of PVDF membranes. Analysis of CA and FE-SEM proved improvement of hydrophilic property of charge-modified membranes without significant change of its morphology. Surface charge characteristics of charge-modified membranes were detected by IEC and zeta potential, detected by ELS. Positively charged PVDF-PHPG membrane has positive zeta potential value at pH range of 3-10. Zeta potential value of neutral charged PVDF-HPG membrane is between 0-10 and that value of negatively charged PVDF-NHPG membrane was below –30. Protein filtration test using BSA (negatively charged) or Lyz (positively charged) dissolved PBS solution

(pH 7.4), were performed to detect antifouling property of charged membrane. After 3rd cycles of lysozyme (positively charged) solution filtration, order of flux recovery ratio (FRR) was; positively charged PVDF-PHPG membrane (57%) > neutral charged PVDF-HPG membrane (49.1%) > negatively charged PVDF-NHPG membrane (41.8%) > neat-PVDF membrane (31.4%). At BSA (negatively charged) solution filtration, FRR was; negatively charged PVDF-NHPG membrane (83.3%) > neutral charged PVDF-HPG membrane (75.9%) > neat-PVDF membrane (70.1%) > positively charged PVDF-PHPG membrane (67.3%). Therefore, due to electrostatic repulsion, anti-fouling performance of positively or negatively charged hydrophilic membrane was good at co-ion protein solution and that of neutral charged membrane was intermediate. Furthermore, protein separation was observed by electrostatic interaction, occurred between oppositely charged membrane surface and proteins. As a result, charge-modified PVDF membranes can be used at application of abundant specific charged foulants included wastewater treatment and charged particle-separation application.

5. References

[1] Du, J. R.; Peldszus, S.; Huck, P. M.; Feng, X., Modification of poly (vinylidene fluoride) ultrafiltration membranes with poly (vinyl alcohol) for fouling control in drinking water treatment. *Water research* **2009,** *43* (18), 4559-4568.

[2] Shi, Q.; Su, Y.; Zhao, W.; Li, C.; Hu, Y.; Jiang, Z.; Zhu, S., Zwitterionic polyethersulfone ultrafiltration membrane with superior antifouling property. *Journal of Membrane Science* **2008,** *319* (1), 271-278.

[3] Yang, Y.-F., L.-S. Wan, and Z.-K. Xu, Surface hydrophilization of microporous polypropylene membrane by the interfacial crosslinking of polyethylenimine. *Journal of Membrane Science*, **2009**. *337*(1), 70-80.

[4] Ersahin, M.E., et al., A review on dynamic membrane filtration: Materials, applications and future perspectives. *Bioresource technology*, **2012**. *122*, 196-206.

[5] Rana, D. and T. Matsuura, Surface modifications for antifouling membranes. *Chemical reviews*, **2010**. *110*(4), p. 2448-2471.

[6] Reddy, A., et al., Surface modification of ultrafiltration membranes by preadsorption of a negatively charged polymer: I. Permeation of water soluble polymers and inorganic salt solutions and fouling resistance properties. *Journal of Membrane Science*, **2003**. *214*(2), 211-221.

[7] Hyun, J., et al., Restriction of biofouling in membrane filtration using a

brush-like polymer containing oligoethylene glycol side chains. *Journal of membrane science*, **2006**. *282*(1), 52-59.

[8] Yong-Hong, Z., Q. Yan-Ling, and P. Dong-Xu, Porous membranes modified by hyperbranched polymers Ⅱ: Effect of the arm length of amphiphilic hyperbranched-star polymers on the hydrophilicity and protein resistance of poly (vinylidene fluoride) membrane. *Journal of Membrane Science*, **2007**. *304*(1-2), 138-147.

[9] Singh, N., et al., Surface modification of microporous PVDF membranes by ATRP. *Journal of membrane science*, **2005**. *262*(1), 81-90.

[10] Wang, P., et al., Plasma-induced immobilization of poly (ethylene glycol) onto poly (vinylidene fluoride) microporous membrane. *Journal of Membrane Science*, **2002**. *195*(1), 103-114.

[11] Huang, C., et al., Electrospun Microfibrous Membranes with Atmospheric-Pressure Plasma Surface Modification for the Application in Dye-Sensitized Solar Cells. *Plasma Processes and Polymers*, **2013**. *10*(11), 938-947.

[12] Pal, S., et al., Evaluation of surface roughness of a plasma treated polymeric membrane by wavelet analysis and quantification of its enhanced performance. *Applied Surface Science*, **2008**. *255*(5), 2504-2511.

[13] Zanini, S., et al., Polyethylene glycol grafting on polypropylene

membranes for anti-fouling properties. *Plasma chemistry and plasma processing*, **2007**. *27*(4), 446-457.

[14] Hester, J., et al., ATRP of amphiphilic graft copolymers based on PVDF and their use as membrane additives. *Macromolecules*, **2002**. *35*(20), 7652-7661.

[15] Cai, T., et al., Poly (vinylidene fluoride) membranes with hyperbranched antifouling and antibacterial polymer brushes. *Industrial & Engineering Chemistry Research*, **2012**. *51*(49), 15962-15973.

[16] Cai, T., et al., Surface-functionalizable membranes of polycaprolactone-click-hyperbranched polyglycerol copolymers from combined atom transfer radical polymerization, ring-opening polymerization and click chemistry. *Journal of Materials Chemistry B*, **2013**. *1*(9), 1304-1315.

[17] Han, M.J., G.N.B. Baroña, and B. Jung, Effect of surface charge on hydrophilically modified poly (vinylidene fluoride) membrane for microfiltration. *Desalination*, **2011**. *270*(1), 76-83.

[18] Ochoa, N., M. Masuelli, and J. Marchese, Development of charged ion exchange resin-polymer ultrafiltration membranes to reduce organic fouling. *Journal of membrane science*, **2006**. *278*(1), 457-463.

[19] Bowen, W.R., T.A. Doneva, and H.-B. Yin, Separation of humic acid from a model surface water with PSU/SPEEK blend UF/NF membranes. *Journal of Membrane Science*, **2002**. *206*(1), 417-429.

[20] Zhan, J., et al., Modification of a membrane surface charge by a low temperature plasma induced grafting reaction and its application to reduce membrane fouling. *Separation science and technology*, **2004**. *39*(13), 2977-2995.

[21] Menon, M.K. and A.L. Zydney, Protein charge ladders: a new technique for studying electrostatic interactions in ultrafiltration systems. *Journal of Membrane Science*, **2001**. *181*(2), 179-184.

[22] Rohani, M.M., A. Mehta, and A.L. Zydney, Development of high performance charged ligands to control protein transport through charge-modified ultrafiltration membranes. *Journal of Membrane Science*, **2010**. *362*(1), 434-443.

[23] Valiño, V., et al., Improved separation of bovine serum albumin and lactoferrin mixtures using charged ultrafiltration membranes. *Separation and Purification Technology*, **2014**. *125*, 163-169.

[24] Matsumoto, H., Y. Koyama, and A. Tanioka, Interaction of organic molecules with weak amphoteric charged membrane surfaces: Effect of interfacial charge structure. *Langmuir*, **2002**. *18*(9), 3698-3703.

[25] Ulbricht, M., Advanced functional polymer membranes. *Polymer*, **2006**. *47*(7), 2217-2262.

[26] Matsumoto, H., Y. Koyama, and A. Tanioka, Interaction of proteins with weak amphoteric charged membrane surfaces: effect of pH. *Journal of Colloid and Interface Science*, **2003**. *264*(1), 82-88.

[27] Schüll, C., et al., Linear-Hyperbranched Graft-Copolymers via

Grafting-to Strategy Based on Hyperbranched Dendron Analogues and Reactive Ester Polymers. *Macromolecules*, **2012**. *45*(15), 5901-5910.

[28] Ji, H., et al., Acid-facilitated debenzylation of *N*-Boc, *N*-benzyl double protected 2-aminopyridinomethyl pyrrolidine derivatives. *Tetrahedron*, **2012**. *68*(5), 1359-1366.

[29] Tziveleka, L.-A., et al., Synthesis and evaluation of functional hyperbranched polyether polyols as prospected gene carriers. *International Journal of Pharmaceutics*, **2008**. *356*(1–2), 314-324.

[30] Wang, G., et al., Biomimetic crystallization of calcium carbonate spherules controlled by hyperbranched polyglycerols. *Journal of Materials Chemistry*, **2008**. *18*(24), 2789-2797.

[31] Leung, P., et al., Preparation of silica nanocomposite anion-exchange membranes with low vanadium-ion crossover for vanadium redox flow batteries. *Electrochimica Acta*, **2013**. *105*, 584-592.

[32] Chen, T.-Y. and J. Leddy, Ion exchange capacity of Nafion and Nafion composites. *Langmuir*, **2000**. *16*(6), 2866-2871.

[33] Li, Y. and T.-S. Chung, Exploration of highly sulfonated polyethersulfone (SPES) as a membrane material with the aid of dual-layer hollow fiber fabrication technology for protein separation. *Journal of Membrane Science*, **2008**. *309*(1–2), 45-55.

[34] Li, Y., et al., Exploration of ionic modification in dual-layer hollow fiber membranes for long-term high-performance protein separation. *AIChE Journal*, **2009**. *55*(2), 321-330.

[35] Sunder, A., et al., Controlled synthesis of hyperbranched polyglycerols by ring-opening multibranching polymerization. *Macromolecules*, **1999**. *32*(13), 4240-4246.

[36] van der Knaap, M., et al., Synthesis and Biological Evaluation of Gramicidin S-Inspired Cyclic Mixed α/β-Peptides. *Chemistry & biodiversity*, **2012**. *9*(11), 2494-2506.

[37] Nikoshvili, L., et al., Selective hydrogenation of 2-methyl-3-butyn-2-ol over Pd-nanoparticles stabilized in hypercrosslinked polystyrene: Solvent effect. *Catalysis Today*, **2014**.

[38] Dzalmukhanova, A., et al., Spectroscopic kinetic study of the interaction of urethanes with amines. *Kinetics and Catalysis*, **2013**. *54*(6), 656-661.

[39] Qiu, F., et al., Synthesis, physical properties and simulation of thermo-optic switch based on azo benzothiazole heterocyclic polymer. *Optical Materials*, **2014**. *36*(7), 1153-1159.

[40] Moussaif, N., et al., XPS analysis of the PC/PVDF interface modified by PMMA. Location of the PMMA at the interface. *Polymer*, **2000**. *41*(9), 3391-3394.

[41] He, F., et al., PVDF film tethered with RGD-click-poly (glycidyl methacrylate) brushes by combination of direct surface-initiated ATRP and click chemistry for improved cytocompatibility. *RSC Advances*, **2014**. *4*(1), 105-117.

[42] Zhao, Y.-H., et al., Achieving highly effective non-biofouling

performance for polypropylene membranes modified by UV-induced surface graft polymerization of two oppositely charged monomers. *The Journal of Physical Chemistry B*, **2010**. *114*(7), 2422-2429.

[43] Kim, K., et al., Evaluation of electroosmosis and streaming potential for measurement of electric charges of polymeric membranes. *Journal of Membrane Science*, **1996**. *116*(2), 149-159.

[44] Qiu, X., et al., Selective separation of similarly sized proteins with tunable nanoporous block copolymer membranes. *ACS nano*, **2012**. *7*(1), 768-776.

[45] Cowan, S. and S. Ritchie, Modified polyethersulfone (PES) ultrafiltration membranes for enhanced filtration of whey proteins. *Separation Science and Technology*, **2007**. *42*(11), 2405-2418.

[46] Saksena, S. and A.L. Zydney, Effect of solution pH and ionic strength on the separation of albumin from immunoglobulins (IgG) by selective filtration. *Biotechnology and bioengineering*, **1994**. *43*(10), 960-968.

[47] Van Reis, R., et al., High-performance tangential flow filtration using charged membranes. *Journal of Membrane Science*, **1999**. *159*(1), 133-142.

[48] Rohani, M.M. and A.L. Zydney, Role of electrostatic interactions during protein ultrafiltration. *Advances in Colloid and Interface Science*, **2010**. *160*(1–2), 40-48.

[49] van Eijndhoven, R.H., S. Saksena, and A.L. Zydney, Protein fractionation using electrostatic interactions in membranel filtration.

Biotechnology and bioengineering, **1995**. *48*(4), 406-414.

[50] Musale, D. and S. Kulkarni, Relative rates of protein transmission through poly (acrylonitrile) based ultrafiltration membranes. *Journal of membrane science*, **1997**. *136*(1), 13-23.

국문초록

본 연구에서는 한외/정밀 (UF/MF)여과 폴리염화비닐리덴 (polyvinylidene fluoride, PVDF)분리막에 양, 중성, 음전하가 도입된 고차가지구조 폴리글리세롤(hyperbranched polyethyleneglycol, HPG)을 공유결합을 이용해 개질하여, 전하를 가지는 분리막을 제조하고, 이를 다양한 전하를 가지는 단백질 용수 처리에 이용하여 오염 저감 효과 및 단백질 분리 성능을 확인하였다. 먼저, 고차가지구조 폴리글리세롤을 중합한 후, 말단기 개질을 이용하여 양, 중성, 음전하를 도입하였다. 분리막의 개질 시, 공경크기 감소를 제어하기 위하여, 상압조건에서의 플라즈마 조사를 실시하여 분리막에 작용기를 도입하였다. 다음으로 가교제와 작용기를 반응시킨 분리막에 전하를 가지는 고차가지구조 폴리글리세롤을 공유결합을 통해 도입하여 양, 중성, 음전하를 가지는 분리막을 제조하였다. HPG 의 성공적인 중합 및 전하 도입 정도는 푸리에

변환 적외선 분광광도계 (FT-IR)와 수소 핵자기 공명 분광 (^{1}H-NMR) 분석을 통해 확인하였으며, 감쇠 전반사 적외선 분광광도계 (ATR-IR)과 광전자 분광기(XPS) 분석에 의하여 분리막 표면에 개질 된 전하를 도입한 HPG 를 정성적, 정량적으로 확인할 수 있었다. 전하 도입 분리막의 친수성 증가는 접촉각(CA)감소를 통해 확인되었고, 주사전자현미경 (FE-SEM)관찰 결과 전하 도입 분리막의 표면구조가 크게 변하지 않은 것이 확인되었다. 전하 도입 분리막의 전하 특성은 이온교환능(IEC)과 제타포텐셜 분석을 통해 관찰하였다. pH 3~10 사이에서 양전하 개질 분리막(PVDF-PHPG)은 10 이상의 제타포텐셜 값을 보였으며, 중성 개질 분리막(PVDF-HPG)은 0~10 사이의 중성값을 보였고, 음전하 개질 분리막은(PVDF-NHPG) -30 이하의 음전하 값을 보였다. 제조된 전하 도입 분리막의 오염 방지능을 확인하기 위하여 양전하를 가지는 오염물질로 대표적인 라이소자임과 음전하를 가지는 오염물질로 대표적인 소혈청 알부민을 포함한 용수를 사용하여

투과평가를 3회에 걸쳐 진행하였다. pH 7.4에서 소수성을 가지는 순수 PVDF 분리막과 PVDF-NHPG 분리막을 이용한 라이소자임 용액 투과 실험 후, 유사한 음의 제타포텐셜 값을 가지지만 친수성이 증가된 PVDF-NHPG 분리막이 오염저감 효과가 높은 것을 확인했다. 그리고 분리막과 오염물간의 전기적 상호작용에 의하여 양전하를 가진 라이소자임 용액 투과 시에는 PVDF-PHPG 분리막이, 소혈청 알부민 용액 투과 시에는 PVDF-NHPG 분리막의 총 오염 (Rt)과 비가역 오염 (Rir)이 가장 적은 것을 확인하였다. 분리막 표면전하와 반대되는 전하를 가지는 단백질의 흡착효과에 의하여 단백질 선택도 증가에 의한 분리 가능성도 확인하였다. 따라서 상기 분리막은 공유결합에 의한 전하의 도입에 의하여 투과 중 도입물의 탈착이 일어나지 않아 환경친화적이며, 특정 전하를 가지는 오염물이 많은 하수 처리 시 오염 저항 효과가 나타나므로 장기간 사용이 가능할 것이며 전하를 띄는 입자의 분리에도 사용 가능할 것으로 예측된다.